



Deposited via The University of Sheffield.

White Rose Research Online URL for this paper:

<https://eprints.whiterose.ac.uk/id/eprint/218461/>

Version: Published Version

Article:

Aad, G., Aakvaag, E., Abbott, B. et al. (2024) Search for pair-produced vectorlike quarks coupling to light quarks in the lepton plus jets final state using 13 TeV pp collisions with the ATLAS detector. *Physical Review D*, 110 (5). 052009. ISSN: 2470-0010

<https://doi.org/10.1103/physrevd.110.052009>

Reuse

This article is distributed under the terms of the Creative Commons Attribution (CC BY) licence. This licence allows you to distribute, remix, tweak, and build upon the work, even commercially, as long as you credit the authors for the original work. More information and the full terms of the licence here:

<https://creativecommons.org/licenses/>

Takedown

If you consider content in White Rose Research Online to be in breach of UK law, please notify us by emailing eprints@whiterose.ac.uk including the URL of the record and the reason for the withdrawal request.

Search for pair-produced vectorlike quarks coupling to light quarks in the lepton plus jets final state using 13 TeV pp collisions with the ATLAS detector

G. Aad *et al.**
(ATLAS Collaboration)

 (Received 31 May 2024; accepted 8 August 2024; published 24 September 2024)

A search is presented for the pair production of heavy vectorlike quarks (VLQs) that each decay into a W boson and a light quark. This study focuses on events where one W boson decays into leptons and the other into hadrons. The search analyzed 140 fb^{-1} of pp collision data with $\sqrt{s} = 13 \text{ TeV}$, recorded by the ATLAS detector from 2015 to 2018 during run 2 of the Large Hadron Collider. The final state is characterized by a high-transverse-momentum isolated electron or muon, large missing transverse momentum, multiple small-radius jets, and a single large-radius jet identified as originating from the hadronic decay of a boosted W boson. With higher center-of-mass energy and integrated luminosity than in the run 1 search, and improved analysis tools, this analysis excludes VLQs (Q) with masses below 1530 GeV at 95% confidence level for the branching ratio $\mathcal{B}(Q \rightarrow Wq) = 1$, an improvement of 840 GeV on the previous ATLAS limit.

DOI: [10.1103/PhysRevD.110.052009](https://doi.org/10.1103/PhysRevD.110.052009)

I. INTRODUCTION

The Standard Model (SM) of particle physics has stood as a highly successful theory for many decades. Despite its successes, the SM falls short in explaining several phenomena, including the matter-antimatter asymmetry, the fermion mass hierarchy, and dark matter. A notable concern within the SM framework is the issue of the Higgs boson's mass divergence [1], which arises from quantum corrections due to interactions with other particles. Various models have emerged to address these shortcomings of the SM, such as top color [2,3], little Higgs [4], composite Higgs [5,6], and the left-right mirror models [7]. A common thread among these models is the introduction of additional particles known as vectorlike quarks (VLQs), for which the left- and right-handed chiralities transform identically under the electroweak gauge group $SU(2) \times U(1)$ [8,9]. These particles may either be composite states linked to the strongly coupled sector or interact with same-charge SM quarks. At the Large Hadron Collider (LHC), a single VLQ can be produced via the electroweak interaction, whereas pair production takes place via the strong interaction. The cross section for pair production depends

only on the VLQ mass, while for single production the cross section depends on the coupling parameter [10–12].

Most past searches have focused on models with VLQs that mix with third-generation quarks, while only a few have considered mixing with lighter generations [13–16]. The previous best lower limit on the mass of new heavy quarks (Q) that decay to light SM quarks is from the CMS Collaboration, using run 1 data [16]. For pair production, VLQs with masses below 845 GeV are excluded for branching ratio $\mathcal{B}(Q \rightarrow Wq) = 1$, and for single production, masses below 685 GeV are excluded for a weak-isospin singlet Q , corresponding to $\mathcal{B}(Q \rightarrow Wq; Zq; Hq) = 0.5:0.25:0.25$ [11]. The previous ATLAS searches for single and pair production of such VLQs were performed at $\sqrt{s} = 7$ and 8 TeV [13,15,17]. In addition, the analysis in Ref. [18] sets even stronger limits by reinterpreting and combining various channels with current LHC measurements to VLQs.

The present search focuses on pair production of VLQs that decay into a W boson and a light quark ($Q\bar{Q} \rightarrow WqWq$, with $q = u, d, \text{ or } s$) using 140 fb^{-1} of pp collisions with $\sqrt{s} = 13 \text{ TeV}$ collected by the ATLAS detector. Figure 1 illustrates a characteristic Feynman diagram for this process. Consequently, this analysis complements the more common searches for top- and bottom-partner VLQs that are assumed to mix only with the third-generation SM quarks [19–23]. The event selection targets the final state where one W boson decays leptonically, which greatly reduces the multijet background, and the other W boson decays hadronically, which

*Full author list given at the end of the article.

Published by the American Physical Society under the terms of the [Creative Commons Attribution 4.0 International license](https://creativecommons.org/licenses/by/4.0/). Further distribution of this work must maintain attribution to the author(s) and the published article's title, journal citation, and DOI. Funded by SCOAP³.

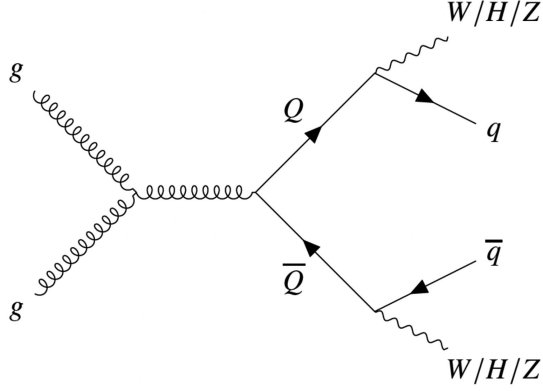


FIG. 1. Illustrative Feynman diagram of pair production of the vectorlike quarks. Each vectorlike quark decays into a light quark and either a W boson, a Z boson, or a Higgs boson.

has a large branching ratio. Events are selected in this channel, requiring a high- p_T charged lepton ($\ell = e$ or μ), missing transverse momentum, and a minimum of three jets (comprising two small-radius jets and a large-radius jet). For better discrimination between signal and background, the search leverages the distinct topology of the high- p_T decay products from the VLQs, particularly the highly boosted W bosons, and the transverse momentum balance between these products. The masses of VLQs where the W bosons decay leptonically ($m_{\text{VLQ}}^{\text{lep}}$) and hadronically ($m_{\text{VLQ}}^{\text{had}}$) are reconstructed from the final-state particles after employing several kinematic requirements to isolate a high-purity sample of signal-like events. The final step involves scrutinizing the number of observed events for any signal-like excess over the SM prediction.

II. ATLAS DETECTOR

The ATLAS experiment [24] at the LHC is a multipurpose particle detector with a forward-backward symmetric cylindrical geometry and a near 4π coverage in solid angle.¹ It consists of an inner tracking detector (ID) surrounded by a thin superconducting solenoid providing a 2 T axial magnetic field, electromagnetic and hadronic calorimeters, and a muon spectrometer. The inner tracking detector covers the pseudorapidity range $|\eta| < 2.5$. It consists of silicon pixel, silicon microstrip, and transition

¹ATLAS uses a right-handed coordinate system with its origin at the nominal interaction point (IP) in the center of the detector and the z -axis along the beam pipe. The x -axis points from the IP to the center of the LHC ring, and the y -axis points upward. Polar coordinates (r, ϕ) are used in the transverse plane, (ϕ) being the azimuthal angle around the z -axis. The pseudorapidity is defined in terms of the polar angle (θ) as $\eta = -\ln(\theta/2)$ and is equal to the rapidity $y = \frac{1}{2} \ln\left(\frac{E+p_z c}{E-p_z c}\right)$ in the relativistic limit. Angular distance is measured in units of $\Delta R \equiv \sqrt{(\Delta y)^2 + (\Delta \phi)^2}$.

radiation tracking detectors. Lead/liquid-argon (LAr) sampling calorimeters provide electromagnetic (EM) energy measurements with high granularity within the region $|\eta| < 3.2$. A steel/scintillator-tile hadronic calorimeter covers the central pseudorapidity range ($|\eta| < 1.7$). The end cap and forward regions are instrumented with LAr calorimeters for EM and hadronic energy measurements up to $|\eta| = 4.9$. The muon spectrometer surrounds the calorimeters and is based on three large superconducting air-core toroidal magnets with eight coils each. The field integral of the toroids ranges between 2.0 and 6.0 Tm across most of the detector. The muon spectrometer includes a system of precision tracking chambers up to $|\eta| = 2.7$ and fast detectors for triggering up to $|\eta| = 2.4$. The luminosity is measured mainly by the LUCID-2 [25] detector, which is located close to the beam pipe. A two-level trigger system is used to select events [26]. The first-level trigger is implemented in hardware and uses a subset of the detector information to accept events at a rate below 100 kHz. This is followed by a software-based trigger that reduces the accepted event rate to 1 kHz on average depending on the data-taking conditions. A software suite [27] is used in data simulation, in the reconstruction and analysis of real and simulated data, in detector operations, and in the trigger and data acquisition systems of the experiment.

III. DATA AND SIMULATED EVENT SAMPLES

The analysis uses the ATLAS run 2 data collected during 2015–2018, with an integrated luminosity of $140.1 \pm 1.2 \text{ fb}^{-1}$ [25,28] from pp collisions at a center-of-mass energy of $\sqrt{s} = 13 \text{ TeV}$. Data quality requirements [29] were applied while choosing the events to be analyzed. These requirements include stable-beam conditions with all detector subsystems and relevant components operational while recording the data.

Monte Carlo (MC) simulated event samples are used to model the background and signal events. All samples were produced using the ATLAS simulation infrastructure [30] and Geant4 [31] to simulate the response of the detector. Data-driven corrections were applied to simulated $W + \text{jets}$, $t\bar{t}$, single-top and multijet events, while all other processes were estimated in a purely MC-driven way. The effects of pileup, which refers to additional proton-proton interactions in an event, were modeled by overlaying the hard-scattering events with minimum-bias events, simulated using the soft QCD processes of PYTHIA 8.186 [32] with the A3 set of tuned parameters (“tune”) [33]. Differences between the pileup conditions in data and simulation are taken into account by reweighting the mean number of interactions per bunch crossing in simulation to the one observed in data.

Signal samples simulating pair-produced vectorlike quarks $Q\bar{Q}$ were generated at leading order (LO) with MadGraph 5 [34] using the NNPDF3.0NLO [35] parton distribution function (PDF) set, and interfaced with PYTHIA 8.186

to model the parton shower, hadronization, and underlying event. The samples were produced for the weak-isospin singlet model in the narrow-width approximation with masses from 800 GeV to 2 TeV, in steps of 100 GeV. Dedicated signal samples were also produced for a VLQ from a weak-isospin doublet for the 1.2 TeV mass point and used to confirm that kinematic differences between the singlet and doublet models have a negligible effect on the results. The final results are also tested for other branching ratio scenarios by performing event-by-event reweighting using the generator's decay information. The signal sample cross sections were calculated with TOP++ 2.0 [36] at next-to-next-to-leading order (NNLO) in QCD including the resummation of next-to-next-to-leading logarithmic soft-gluon terms.

The production of a single W boson in association with jets is the dominant background. The production of V + jets ($V = W, Z$) was simulated with the Sherpa 2.2.11 [37] generator using next-to-leading-order (NLO) matrix elements for up to two partons, and LO matrix elements for up to five partons, calculated with the Comix [38] and OpenLoops [39–41] libraries. They were matched with the Sherpa parton shower [42] using the MEPS@NLO prescription [43–46] and the set of tuned parameters developed by the Sherpa authors. The NNPDF3.0NNLO [35] PDF set was used and the samples were normalized to a NNLO prediction [47]. Generator-level W + jets samples were also produced with the Catani-Krauss-Kuhn-Webber (CKKW) merging/matching scale shifted from 20 to 15 GeV or 30 GeV, or with the resummation scale (QSF) parameters varied from 1 to 0.25 or 4, to estimate the related uncertainties.

The production of $t\bar{t}$ events was modeled using the POWHEG BOX[v2] [48–51] generator at NLO with the NNPDF3.0NLO PDF set and the h_{damp} parameter² set to $1.5 m_{\text{top}}$ [52]. The events were interfaced to PYTHIA 8.230 to model the parton shower, hadronization, and underlying event, with parameter values set according to the A14 tune [53] and using the NNPDF2.3LO set of PDFs [54]. The impact of using a different parton shower and hadronization model was evaluated by replacing PYTHIA 8.230 with Herwig 7.0 [55,56], using the H7UE tune [56] and the MMHT2014LO PDF set [57]. To assess the uncertainty in the matching of NLO matrix elements to the parton shower, the POWHEG sample was compared with a sample of events generated with MadGraph5_aMC@NLO 2.6.0 [58] interfaced with PYTHIA 8.230. The MadGraph5_aMC@NLO calculation used the NNPDF3.0NLO PDF set, and PYTHIA 8 used the NNPDF2.3LO PDF set with the A14 tune. The potential impact of underestimating the amount of initial-state radiation (ISR) is assessed by comparing the nominal

²The h_{damp} parameter is a resummation damping factor and one of the parameters that control the matching of POWHEG matrix elements to the parton shower and thus effectively regulates the high- p_T radiation against which the $t\bar{t}$ system recoils.

sample with another that increases the h_{damp} value to $3 m_{\text{top}}$, halves the renormalization and factorization scales, and utilizes the “Var3cUp” weight from the A14 tune. Conversely, a possible overestimation of the amount of ISR is examined by doubling the renormalization and factorization scales in another sample and selecting the “Var3cDown” weight from the A14 tune. Additionally, the uncertainty related to modeling of final-state radiation (FSR) is evaluated by either doubling or halving the renormalization scale for emissions from the parton shower.

Background events may also originate from the production of single-top-quark events. The main contribution to this background comes from top quarks associated with a W boson (tW), while t - and s -channel single-top production gives only a minor contribution. The single-top background was modeled by the POWHEG BOX[v2] [49–51,59] generator at NLO in QCD using the five-flavor scheme and the NNPDF3.0NLO set of PDFs. The events were interfaced with PYTHIA 8.230, which used the A14 tune. Comparisons with samples generated by MadGraph5_aMC@NLO 2.6.2 at NLO in QCD are used to estimate the uncertainty in the matching of NLO matrix elements to the parton shower. The parton shower and hadronization uncertainties are evaluated from comparisons with samples generated with an alternative showering program, Herwig 7.04, using the H7UE tune and the MMHT2014LO PDF set. For the tW samples, the diagram removal (DR) scheme [60] was used to remove interference and overlap with $t\bar{t}$ production. The related uncertainty was estimated by comparing these samples with an alternative sample generated using the diagram subtraction (DS) scheme [52,60].

The contributions from other processes are nearly negligible relative to the overall background. The largest additional background contribution comes from the production of two bosons, either two vector bosons (VV) or a vector boson and a Higgs boson (VH), with at least one lepton in the final state. Diboson events with multiple leptons in the final state are strongly disfavored by requiring exactly one reconstructed lepton in the final state. The VV samples were generated with Sherpa[2.2.2], whereas the VH samples were generated with PYTHIA 8.186. Fully leptonic final states and semileptonic final states, where one boson decays leptonically and the other hadronically, were generated using matrix elements at NLO accuracy in QCD for up to one additional parton and at LO accuracy for up to three additional parton emissions. Samples for the loop-induced $gg \rightarrow VV$ processes were generated using LO-accurate matrix elements for up to one additional parton emission for both the fully leptonic and semileptonic final states. The MEPS@NLO prescription was used to match and merge the matrix element calculations with the Sherpa parton shower based on Catani-Seymour dipole factorization [38,42]. The virtual QCD corrections were provided by the OpenLoops library. The NNPDF3.0NNLO set of PDFs was used, along with a dedicated set of tuned

parton-shower parameters developed by the Sherpa authors. Finally, production of $t\bar{t}V$ events was modeled using the MadGraph5_aMC@NLO 2.3.3 generator at NLO with the NNPDF3.0NLO PDFs, interfaced to PYTHIA 8.210 using the A14 tune and the NNPDF2.3LO PDF set. Multijet events were simulated using the Sherpa[2.1.1] generator with the default CT10 PDF set [61].

IV. OBJECT RECONSTRUCTION

Electrons are reconstructed from energy clusters in the EM calorimeter matched with ID tracks. Electron candidates must be located in the central region of the detector ($|\eta| < 2.47$), have $p_T > 27$ GeV, and be matched to a track with $|z_0 \sin \theta| < 0.5$ mm and $|d_0/\sigma_{d_0}| < 5$, where d_0 is the track's transverse impact parameter with respect to the hard-scatter vertex and its uncertainty is given by σ_{d_0} , and z_0 is its longitudinal impact parameter. Candidates in the transition region between the EM calorimeter's barrel and end cap sections ($1.37 < |\eta| < 1.52$) are excluded. A “baseline electron” selection requires electrons to satisfy the *Medium* likelihood identification criteria with no selection on the isolation. Alternatively, a “tight electron” selection requires satisfying the *Tight* likelihood identification criteria, with loose isolation requirements [62]. The first isolation requirement is $E_{T,\text{cone}}^{\text{isol}}/p_T^e < 0.2$, where p_T^e is the electron candidate's p_T , and $E_{T,\text{cone}}^{\text{isol}}$ is the energy deposited in the calorimeter within a cone of angular size $\Delta R = 0.2$ around the candidate's direction, with energy leakage and pileup contributions subtracted. The second requirement is $p_{T,\text{var}}^{\text{isol}}/p_T^e < 0.15$, where $p_{T,\text{var}}^{\text{isol}}$ is the sum of the track p_T , excluding the electron candidate, within a cone of size $\Delta R = \min(0.2, 10 \text{ GeV}/p_T^e)$. Data-based scale factors [62] are employed to correct for variations in reconstruction, identification, isolation, and trigger efficiencies between data and simulation.

Muons are reconstructed [63] using combined tracks in the MS and the ID. Baseline muons must meet *Loose* identification criteria with no isolation requirements, while tight muons must satisfy *Tight* identification criteria [63] and meet the track-based isolation requirements defined by the “TightTrackOnly” working point. This working point uses the scalar sum of the p_T of all tracks that are within a cone of size $\Delta R = \min(0.3, 10 \text{ GeV}/p_T^\mu)$ around the muon candidate, where p_T^μ is the muon candidate's p_T . The track matched to the muon candidate under consideration is excluded from the sum. The muon is selected if this sum is less than 6% of p_T^μ . All muon candidates must also satisfy $|z_0 \sin \theta| < 0.5$ mm and $|d_0/\sigma_{d_0}| < 3$. Muons are required to have $p_T > 25$ GeV and a reconstruction limit of $|\eta| < 2.5$. Efficiency scale factors are applied to account for differences in muon reconstruction, identification, vertex association, isolation, and trigger efficiencies between simulation and data [63].

Small-radius (small- R) jet candidates are formed from particle-flow objects [64], utilizing the anti- k_t algorithm [65,66] with a radius parameter of $R = 0.4$. The particle-flow algorithm combines information from ID tracks and calorimeter energy deposits to construct input for jet reconstruction. The jet energy is calibrated to the particle scale, i.e. without detector effects, through a series of corrections, including simulation-based adjustments and *in situ* calibrations [67]. Jets are required to have $p_T > 25$ GeV and $|\eta| < 2.5$. To reject jets originating from pileup interactions, jet candidates with $|\eta| < 2.4$ and $20 < p_T < 60$ GeV must satisfy the tight jet-vertex-tagger (JVT) criterion [68]. Small- R jets containing a b -hadron decay are identified using the DL1r algorithm [69]. Jets are considered b -tagged if they meet the operating point criteria for 70% efficiency [70]. The b -tagging efficiencies in simulation, as well as the charm and light mistag rates, are corrected to match those in data [71,72].

Large-radius (large- R) jets are constructed from noise-suppressed topological calorimeter-cell clusters with the anti- k_t algorithm with a radius parameter of $R = 1.0$, and calibrated using local hadronic cell reweighting [73]. These large- R jets are required to have $p_T > 200$ GeV and $|\eta| < 2$.

A W -boson tagging algorithm identifies high- p_T hadronically decaying W bosons that produce a single collimated large- R jet [74], with 80% efficiency. It uses criteria based on the mass of the large- R jet, the number of ID tracks associated with the jet, and the energy correlation function ratio D_2 [74,75]. Scale factors adjust the W -boson tagging efficiency in simulation to match that in data [76].

The missing transverse momentum is calculated as the negative vectorial sum of the transverse momenta of all the calibrated objects in an event, augmented by a track-based soft term that accounts for energy depositions linked to the event's primary vertex but not attributed to any calibrated object [77]. The magnitude of the missing transverse momentum is denoted by E_T^{miss} and is required to exceed 250 GeV. In signal events, a significant amount of E_T^{miss} is expected from the boosted leptonically decaying W boson.

An overlap removal procedure, based on the baseline lepton definitions, is employed to avoid double counting of ambiguous reconstructed objects. First, electron-muon overlap is addressed by removing any muon that shares a track in the ID with an electron if the muon is only “calorimeter-tagged” (because of poor MS acceptance at $|\eta| \approx 0$), or otherwise removing the electron. Subsequently, overlap between jets and leptons is resolved by rejecting any jets within $\Delta R = 0.2$ of an electron and then rejecting any electrons within $\Delta R = 0.4$ of a jet. Similarly, jets are rejected if they have fewer than three associated tracks and are within $\Delta R = 0.2$ of a muon candidate; otherwise, the muon is rejected if it lies within $\Delta R = \min(0.4, 0.004 + 10 \text{ GeV}/p_T^\mu)$ of a jet.

An additional procedure to resolve overlaps between small- R jets and large- R jets is described in Sec. V.

TABLE I. Common preselection criteria for all analysis regions.

= 1 isolated lepton ($\ell = e$ or μ) with $p_T^\ell \geq 60$ GeV
$E_T^{\text{miss}} \geq 250$ GeV
≥ 1 large- R jet with $p_T \geq 200$ GeV
≥ 2 small- R jets with $p_T \geq 25$ GeV
≥ 1 small- R jet with $p_T \geq 200$ GeV
$\Delta R(\text{small-}R \text{ jets}, W_{\text{had}}) > 1.0$

V. EVENT SELECTION

This analysis focuses on the VLQ pair decay $Q\bar{Q} \rightarrow WqWq$ with one W boson decaying leptonically and the other hadronically. A single-lepton trigger [78,79] was used and events selected with this trigger were required to have exactly one electron with $p_T \geq 27$ GeV or one muon with $p_T \geq 25$ GeV. In addition to this, at least three small- R jets with $p_T \geq 25$ GeV, and $E_T^{\text{miss}} \geq 250$ GeV, are required. These basic event-level requirements ensure the identification of at least one quark from a hadronically decaying W boson, two additional quarks coming directly from the two VLQ decays, and one leptonically decaying W boson.

Events must satisfy a series of criteria referred to as the ‘‘preselection’’ that significantly reduce the background while retaining events consistent with the signal process. As summarized in Table I, the preselection requires exactly one charged lepton, large E_T^{miss} , at least one large- R jet, and at least two small- R jets. Events passing preselection have two reconstructed W candidates. The leptonically decaying W boson (W_{lep}) is reconstructed by combining the lepton and the reconstructed neutrino; where the neutrino is reconstructed using the event’s E_T^{miss} and the z -component of the neutrino’s momentum, estimated by using the mass of the W boson as a constraint. The hadronically decaying W boson (W_{had}), is defined as the leading W -tagged large- R jet. If no large- R jet meets the W -tagging criteria, then the W_{had} candidate is defined to be the large- R jet closest in mass to the W boson [80]. Finally, an additional overlap removal procedure requires small- R jets to be separated from the W_{had} candidate by $\Delta R \geq 1.0$. Small- R jets that fail this requirement are removed from the analysis and thus not considered in the reconstruction of the VLQs.

The input for the VLQ pair reconstruction algorithm consists of the W_{had} and W_{lep} and the small- R jets after overlap removal. The three leading small- R jets are then paired with the reconstructed W bosons, and for each pairing the invariant mass of each VLQ candidate is computed. The pairing resulting in the smallest mass difference $|m_{\text{VLQ}}^{\text{lep}} - m_{\text{VLQ}}^{\text{had}}|$ is chosen.

Events that pass the preselection are then categorized into signal regions (SRs), reweighting regions (RwRs), and validation regions (VRs). These regions are orthogonal, and the RwRs and VRs are chosen to be kinematically close to

the SRs. The SRs are designed to maximize the sensitivity to the possible presence of signal events. The RwRs have high purity for a particular SM process and are used to calculate data-driven corrections for that process. The VRs are also dominated by a single SM process and are used to validate the MC simulation’s modeling of the data after corrections. Kinematic requirements for the variables defining the SRs are chosen to optimize S/\sqrt{B} for a signal mass of 1400 GeV, since this is close to the expected mass reach of the analysis for signal events in the $WqWq$ decay channel.

Two signal regions, SR1 and SR2, are defined for this analysis. Using two SRs increases the sensitivity since SR1 has a higher S/\sqrt{B} than when using a single SR combining SR1 and SR2. Events in either SR must have zero b -tagged small- R jets, at least one W -tagged large- R jet, $\Delta\phi(\text{lepton}, E_T^{\text{miss}}) \leq 0.5$, $\Delta R(W_{\text{lep}}, W_{\text{had}}) \geq 0.8$, and $S_T \geq 2000$ GeV, where S_T is the scalar sum of the E_T^{miss} and the transverse momenta of the charged lepton and selected small- R jets. This variable has higher discriminating power due to the large expected mass of the VLQ. A final requirement separates the events into either SR1 or SR2. SR1 requires $\Delta\phi(\text{lead jet}, E_T^{\text{miss}}) < 2.75$, resulting in a higher S/\sqrt{B} . SR2 requires $\Delta\phi(\text{lead jet}, E_T^{\text{miss}}) \geq 2.75$, selecting signal events not assigned to SR1, at the expense of a small contribution from multijet events.

Three reweighting regions, $WRwR$, $t\bar{t}RwR$, and multijetRwR, are used to correct for mismodeling in the $W + \text{jets}$ [81], $t\bar{t}$ plus single-top, and multijet background predictions, respectively. In addition, the validation regions WVR , $t\bar{t}VR$, and multijetVR are defined in order to validate the modeling of the $W + \text{jets}$, $t\bar{t}$, and multijet backgrounds in independent regions. Kinematic requirements for the SRs, RwRs, and VRs are summarized in Table II in addition to the usage of region in the fit model of the statistical analysis. The normalization of the multijet MC samples is determined using multijetRwR. Both $t\bar{t}RwR$ and $WRwR$ are used to correct the normalization and shape of the respective MC event distributions.

VI. BACKGROUND ESTIMATION

The background for this analysis is primarily due to $W + \text{jets}$ events, followed by $t\bar{t}$ and single-top events. Except for these and the multijet backgrounds, all other backgrounds such as $Z + \text{jets}$, ttV , and diboson (VV and VH) events are combined due to their small contributions and labeled as ‘‘Other Bkgs.’’ These other backgrounds are estimated purely from the MC simulations. Utilizing the RwRs described above, reweighting factors are derived for $W + \text{jets}$ events, multijet events, and the combined $t\bar{t}$ plus single-top events. This reweighting is performed to correct the normalization and shape of the S_T distribution for the $W + \text{jets}$ and $t\bar{t}$ plus single-top events. The reweighting is determined by fitting the ratio of the observed data, after

TABLE II. Selection criteria for the two signal regions and three reweighting and validation regions used in the analysis.

Variable	SR1 (SR2)	MultijetRwR	MultijetVR	WRwR	WVR	$t\bar{t}$ RwR	$t\bar{t}$ VR
$N_{b\text{-tags}}$	= 0	= 0	= 0	= 0	= 0	≥ 1	≥ 1
$N_{W\text{-tags}}$	≥ 1	= 0	≥ 1	= 0	> 0	≥ 1	= 0
$\Delta R(W_{\text{lep}}, W_{\text{had}})$	≥ 0.8	< 0.8	< 0.8	≥ 0.8	< 0.8	< 0.8	≥ 0.8
$\Delta\phi(\text{lepton}, E_{\text{T}}^{\text{miss}})$	≤ 0.5	≤ 0.1	≤ 0.1		> 0.1		
S_{T}	≥ 2000 GeV						
$\Delta\phi(\text{leading jet}, E_{\text{T}}^{\text{miss}})$	< 2.75 (≥ 2.75)						
Included in fit	Yes	No	No	No	No	No	No

subtracting the SM predictions for processes other than the one being corrected, to the prediction for the process being corrected. A normalization reweighting factor is derived for the multijet background, while the normalization and shape reweightings for $W + \text{jets}$ events and the combined $t\bar{t}$ plus single-top events pertain to their S_{T} distributions, with the above-described ratio fitted to a function of form

$$f(S_{\text{T}}) = P_0 + \exp(P_1 S_{\text{T}}), \quad (1)$$

where P_0 and P_1 are the fitted parameters. The reweightings are derived in an iterative procedure, which terminates when all reweightings change by less than 1% from the previous iteration. In the first step of the first iteration, the multijet normalization reweighting is derived in the multijetRwR. In the second step of the first iteration, the previously derived multijet reweighting is applied to multijet events and then the $t\bar{t}$ RwR is used to derive the reweighting function for $t\bar{t}$ and single-top events. For the last step of the first iteration, the previously derived reweightings are applied to the multijet events and the $t\bar{t}$ and single-top events, and the reweighting for the

$W + \text{jets}$ background is derived in the WRwR and applied to the $W + \text{jets}$ events. These steps are repeated in the next iteration. However, at the start of each step of this iteration, only reweightings derived for samples other than the one under consideration are applied to the relevant samples. The previously derived reweighting for the sample under consideration in the step is not used. For example, in the first step of the second iteration, the multijet normalization reweighting is rederived, but with only the reweightings obtained for $t\bar{t}$ plus single-top and $W + \text{jets}$ from the first iteration applied to the $t\bar{t}$, single-top, and $W + \text{jets}$ samples. This procedure was found to converge after just two iterations, and a third iteration produced reweighting factors almost identical to those obtained in the second iteration.

Figure 2 shows the S_{T} distribution in the WRwR and $t\bar{t}$ RwR after applying the reweighting for $W + \text{jets}$, $t\bar{t}$, and multijet events as determined in their respective reweighting regions. The red marker in the data-to-background ratio represents the ratio before the reweighting is applied, whereas the black marker represents the ratio after the reweighting is applied. The derived reweighting factors

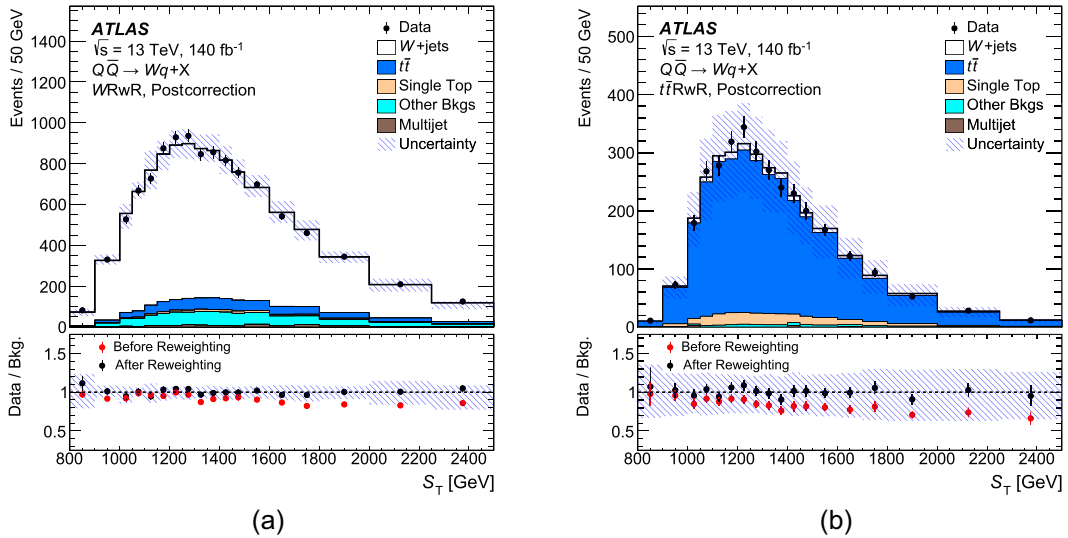


FIG. 2. Reconstructed S_{T} distribution in the (a) WRwR and (b) $t\bar{t}$ RwR after applying the reweighting corrections. The uncertainty band includes all systematic uncertainties, as described in detail in Sec. VII. The lower panel shows the ratio of data to the SM prediction before (red points) and after (black points) applying the reweighting corrections.

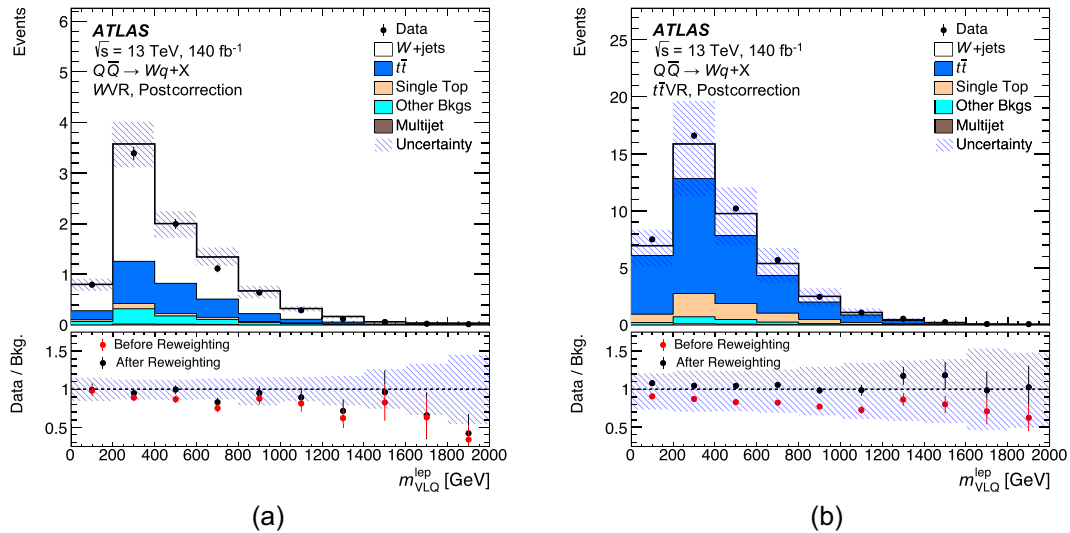


FIG. 3. Reconstructed mass distribution of leptonically decaying VLQ candidates in the (a) WVR and (b) $t\bar{t}VR$ after applying the reweighting corrections. The uncertainty band includes all systematic uncertainties, as described in detail in Sec. VII. The lower panel shows the ratio of data to the SM prediction before (red points) and after (black points) applying the reweighting corrections.

improve the modeling in the high- S_T regions. The mass of leptonically decaying VLQ candidates is used as a discriminating variable in the final likelihood fit. Improvement in modeling is further validated in Fig. 3 by plotting this discriminating variable, m_{VLQ}^{lep} , in the respective VRs for $W + \text{jets}$ and $t\bar{t}$ backgrounds after applying the reweighting and showing the data/MC ratios before and after the reweighting.

VII. SYSTEMATIC UNCERTAINTIES

Systematic uncertainties can be categorized into two main types: modeling uncertainties and experimental uncertainties. Modeling uncertainties encompass uncertainties related to the modeling of specific physical processes and the parameters chosen within those models. These uncertainties are often related to calculations and assumptions in the underlying theory. Experimental uncertainties concern detector setup, the modeling of the detector's response to the various objects, and the uncertainties in the data-driven corrections.

The uncertainty in the combined 2015–2018 integrated luminosity is 0.83% [28], obtained using the LUCID-2 detector [25] for the primary luminosity measurements. Pileup corrections are performed by adjusting the pileup distribution in simulated data to match the real data. Uncertainties are then calculated by varying the correction.

Uncertainties related to electron and muon energy-scale calibration and resolution, and electron and muon reconstruction, identification, and isolation efficiencies are considered [62,63,82]. Variations are also applied to account for uncertainties in the muon spectrometer's track resolution and momentum scale.

Uncertainties in the jet energy scale and jet energy resolution [67] are taken into account for both small- R jets and large- R jets. In addition, the jet mass scale [83] and jet mass resolution [84] are considered for both the small- R and large- R jets. The systematic uncertainty associated with the JVT requirement is estimated by varying the scale factor used to raise or lower the JVT efficiency in simulation within its uncertainties.

The b -tagging efficiency corrections include uncertainties from the b -tagged-jet selection. An uncertainty in extrapolating of the b -tagging efficiency calibration to high jet p_T is considered. Systematic uncertainties in the W -tagging efficiency and inefficiency corrections are applied [74].

Uncertainties in data-driven corrections to simulated events, as described in Sec. VI for processes such as multijets and $t\bar{t}$, are considered in the analysis. For $t\bar{t}$ and $W + \text{jets}$, two shape uncertainties apply to the calculated reweighting corrections, corresponding to uncertainties in the P_0 and P_1 parameters of the function $f(S_T) = P_0 + \exp(P_1 S_T)$ introduced in Eq. (1). A uniform 40% normalization uncertainty is assigned to $t\bar{t}$ events based on the prefit uncertainty at high S_T for these events. The limit is not sensitive to the normalization of $W + \text{jets}$ so it is included as a free parameter in the final fit.

Uncertainties due to the choice of QCD scales are estimated for the main backgrounds, from $W + \text{jets}$, $t\bar{t}$, and single-top events. These uncertainties are evaluated with a six-point variation of the chosen renormalization and factorization scales, evaluated by either doubling or halving each, or both, from the nominal values. The uncertainty due to the choice of PDF is estimated by using alternative PDFs and also the PDF4LHC15 combined PDF set [85]. For the $W + \text{jets}$ samples, the uncertainties associated with

matching the matrix elements to the parton showers, and merging different jet multiplicities into an inclusive sample, are estimated from comparisons between the samples with altered CKKW merging/matching scales and QSF parameter values listed in Sec. III.

The effects of using an alternative MC generator, ISR and FSR model, parton shower model, and shower matching scheme are estimated by comparing the nominal $t\bar{t}$ sample with alternative samples, as explained in Sec. III. Similar uncertainties were evaluated for the single-top events. In addition, the uncertainty due to the choice of scheme to eliminate interference and overlap between tW and $t\bar{t}$ production is evaluated by comparing the nominal single-top MC sample produced with the DR scheme with the alternative sample produced with the DS scheme [52,60,86].

The analysis also has a small contribution from the single-top and multijet backgrounds as well as other backgrounds, which include Z + jets, $t\bar{t}V$, and diboson (VV and VH) events. An uncertainty of 10% is assigned to the cross section for the “other backgrounds” sample. Studies showed that varying the uncertainties for the single-top and multijet backgrounds between 10% and 100% had a negligible impact on the VLQ mass limit expected in the absence of a signal, so a conservative uncertainty of 100% is applied to these backgrounds.

All systematic uncertainties are found to have negligible impact on the sensitivity compared to the statistical uncertainty due to the data sample size.

VIII. STATISTICAL ANALYSIS AND RESULTS

The statistical analysis tests for the presence of VLQ pair production by performing a fit over the two SRs. The

fit utilizes the reconstructed mass of the leptonically decaying VLQ, $m_{\text{VLQ}}^{\text{lep}}$, as the fit variable of choice due to the discriminating power provided by the VLQ mass peak not present in SM backgrounds.

The SRs are fitted to maximize a binned likelihood function $\mathcal{L}(\mu, \theta)$. This likelihood function $\mathcal{L}(\mu, \theta)$ is constructed from a product of Poisson probability terms over all bins considered in the analysis. This function depends on the parameter of interest, the signal strength parameter μ , which is a multiplicative factor applied to the theoretical signal production cross section, and θ , a set of nuisance parameters (NPs) which account for the effects of systematic uncertainties on the number of observed signal and background events. The NPs are implemented as Gaussian or log-normal priors in the likelihood. Therefore, the number of events expected in a particular bin depends on the parameters μ and θ . The signal strength μ is determined by $\mu = \sigma^{\text{test}} / \sigma^{\text{theory}}$, where σ^{test} is the cross section for VLQ pair production used in the fit and σ^{theory} is the theoretical prediction. The NPs θ provide variations in the signal and background event counts consistent with systematic uncertainties. The fitted values of θ account for the deviations from the nominal expectation that provides the best fit to data.

To determine the statistical significance of our results, the test statistic q_μ is taken to be the profile likelihood ratio: $q_\mu = -2 \ln(\mathcal{L}(\mu, \hat{\theta}_\mu) / \mathcal{L}(\hat{\mu}, \hat{\theta}))$ where $\hat{\mu}$ and $\hat{\theta}$ are the parameter values that maximize the likelihood function, subject to the condition $0 \leq \hat{\mu} \leq \mu$, and $\hat{\theta}_\mu$ are the NP values that maximize the likelihood function for a given value of μ .

The results of the fit in the two SRs for the background-only hypothesis, which assumes $\mu = 0$, are shown in Fig. 4.

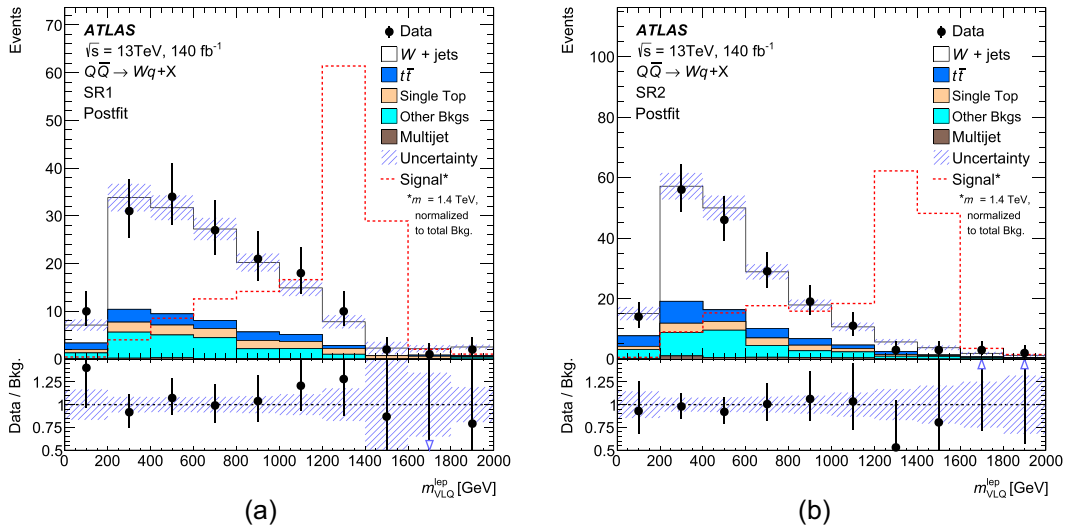


FIG. 4. Distribution for the reconstructed mass of the leptonically decaying VLQ, $m_{\text{VLQ}}^{\text{lep}}$, in (a) SR1 and (b) SR2 after the fit using the background-only hypothesis. For comparison, the shape of the VLQ signal distribution is overlaid for $\mathcal{B}(Q \rightarrow Wq) = 1$ with $m_{\text{VLQ}} = 1400$ GeV and normalized to the total background. The uncertainty bands include all systematic uncertainties described in Sec. VII. An arrow in the bottom panel indicates that the given data point falls outside the range of the plot.

TABLE III. Event yields in the two SRs after the fit to the data under the background-only hypothesis. The uncertainties include statistical and systematic uncertainties.

Process	SR1	SR2
$W + \text{jets}$	104 ± 20	124 ± 23
$t\bar{t}$	13 ± 11	23 ± 15
Single top	11 ± 16	12 ± 15
Other backgrounds	21.3 ± 3.0	30 ± 4
Multijet	0.9 ± 0.9	3.4 ± 3.3
Total	150 ± 10	192 ± 12
Data	156	186

TABLE IV. Expected $Q\bar{Q}$ event yields in the SRs for the scenario $\mathcal{B}(Q \rightarrow Wq) = 1$. The uncertainties include statistical and systematic uncertainties.

m_{VLQ} (GeV)	SR1	SR2
1300	31.0 ± 2.9	15.0 ± 1.2
1400	19.3 ± 2.2	9.4 ± 0.8
1500	11.9 ± 1.7	5.8 ± 0.5

The corresponding yields are listed in Table III. From this fit one can see that the data are in good agreement with the SM background prediction. The expected $Q\bar{Q}$ event yields for three different mass points in the SRs for the scenario $\mathcal{B}(Q \rightarrow Wq) = 1$ are listed in Table IV. To maximize the sensitivity of the search, the two signal regions are combined statistically, allowing the limits on the signal strength to be translated into limits on the total cross section. Upper limits at 95% confidence level (CL) are set on the pair-production cross section for VLQs with masses from 800 to 2000 GeV. Figure 5 shows the results for two benchmark scenarios, one with $\mathcal{B}(Q \rightarrow Wq) = 1$ and the other with $\mathcal{B}(Q \rightarrow Wq:Zq:Hq) = 0.5:0.25:0.25$ in

the SU(2) singlet model. Comparing the observed limits on the cross section with the theory prediction, VLQs with masses below 1530 GeV are excluded for $\mathcal{B}(Q \rightarrow Wq) = 1$ and VLQs with masses below 1150 GeV are excluded for the SU(2) singlet model, while the expected limits for these two cases allow $m_{\text{VLQ}} > 1500$ and 1230 GeV, respectively. This is an improvement of 840 GeV on the previous ATLAS limit [15] and 685 GeV higher than the latest CMS limit [16].

Although this analysis was optimized to search for VLQs that decay into a W boson and a light quark, it also has some sensitivity to signal events with neutral-current decays via a Higgs or Z boson. The sensitivity to Z boson decays is larger given the similarities in the topology of a hadronically decaying Z and W boson. The likelihood of this occurring for a Higgs boson is much lower given the parameters used in the tagging algorithm discussed in Sec. IV. Assuming no other decay modes, the signal MC samples are reweighted to obtain different branching ratio combinations, which can then be used in the final fit. Figure 6 shows 95% CL lower limits on the mass of the VLQ for various branching ratios.

IX. CONCLUSION

A search for the pair production of heavy vectorlike quarks ($Q\bar{Q}$), where each subsequently decays into a W boson and a light quark, was performed using 140 fb⁻¹ of 13 TeV pp collision data recorded with the ATLAS detector during run 2 of the LHC. The analysis specifically targets events in the semileptonic final state, requiring the reconstruction of one leptonically decaying W boson and one hadronically decaying W boson. The final state is characterized by a high-transverse-momentum isolated electron or muon, substantial missing transverse momentum, multiple jets, and a large-radius jet identified as originating from the hadronic decay of a W boson. No

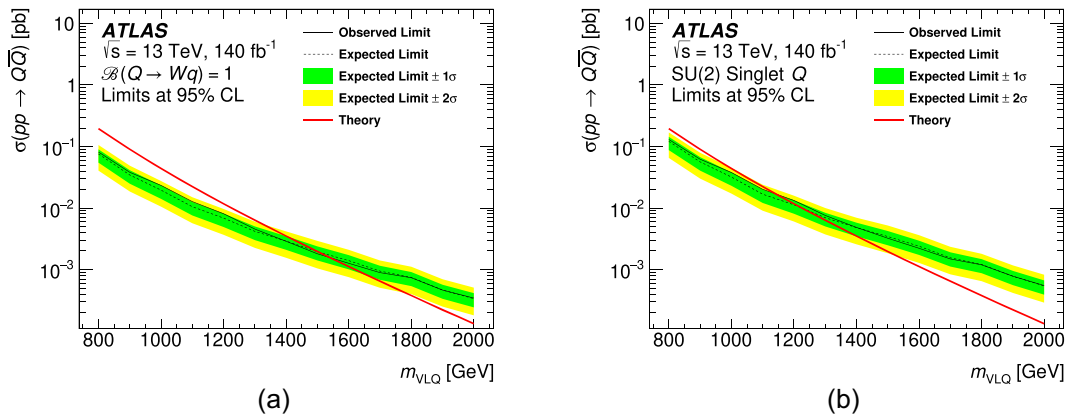


FIG. 5. Expected (dashed black line) and observed (solid black line) 95% CL upper limits on the VLQ pair-production cross section as a function of the VLQ mass for (a) $\mathcal{B}(Q \rightarrow Wq) = 1$ and (b) the SU(2) singlet model. The green and yellow bands correspond to ± 1 and ± 2 standard deviations around the expected limit, respectively. The thin red line shows the theoretical prediction for the given model.

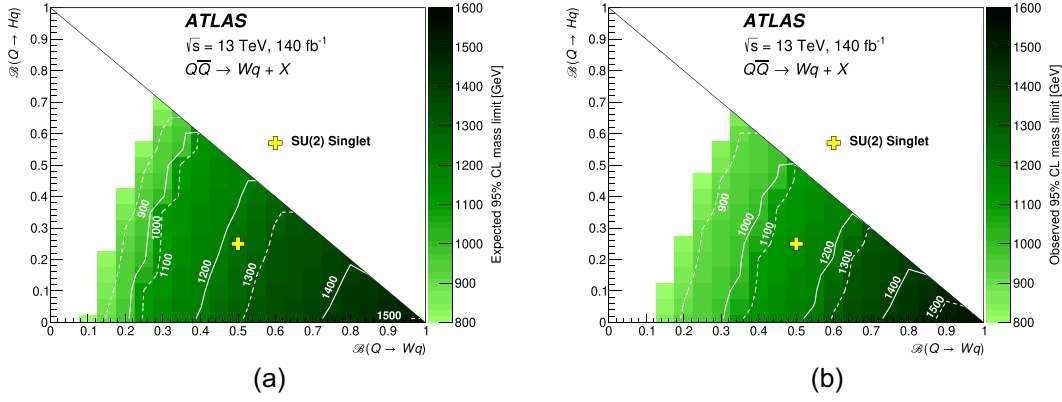


FIG. 6. (a) Expected and (b) observed lower limit on the VLQ mass for various branching ratio (B) configurations at 95% CL. The x -axis shows the branching ratio for decay to a W boson, while the y -axis shows the branching ratio for decay to a Higgs boson. The branching ratio to a Z boson is determined by the requirement that $B(Q \rightarrow Zq) = 1 - B(Q \rightarrow Wq) - B(Q \rightarrow Hq)$. The white region above the solid black line is excluded due to the sum of the individual branching ratios being greater than one. In the white region below this line the lower limit on the VLQ mass is below 800 GeV. The yellow marker indicates the branching ratios for the SU(2) singlet scenario.

significant excess is discovered in the reconstructed vectorlike quark mass distribution, and 95% CL upper limits are derived on the signal production cross section as a function of the vectorlike quark mass. The analysis sets constraints on the mass of the vectorlike quarks for various combinations of their decays to SM bosons and light SM quarks. Notably, masses below 1530 GeV are excluded at 95% CL for $B(Q \rightarrow Wq) = 1$, and masses below 1150 GeV are excluded for the scenario with $B(Q \rightarrow Wq:Zq:Hq) = 0.5:0.25:0.25$. With increased center-of-mass energy and integrated luminosity, as well as improved analysis tools, the exclusion limit for $B(Q \rightarrow Wq) = 1$ is raised by 840 and 685 GeV compared to the run 1 analyses conducted by ATLAS and CMS, respectively.

ACKNOWLEDGMENTS

We thank CERN for the very successful operation of the LHC and its injectors, as well as the support staff at CERN and at our institutions worldwide without whom ATLAS could not be operated efficiently. The crucial computing support from all WLCG partners is acknowledged gratefully, in particular from CERN, the ATLAS Tier-1 facilities at TRIUMF/SFU (Canada), NDGF (Denmark, Norway, Sweden), CC-IN2P3 (France), KIT/GridKA (Germany), INFN-CNAF (Italy), NL-T1 (Netherlands), PIC (Spain), RAL (UK), and BNL (USA), the Tier-2 facilities worldwide, and large non-WLCG resource providers. Major contributors of computing resources are listed in Ref. [87]. We gratefully acknowledge the support of ANPCyT, Argentina; YerPhi, Armenia; ARC, Australia; BMWFW and FWF, Austria; ANAS, Azerbaijan; CNPq and FAPESP, Brazil; NSERC, NRC, and CFI, Canada; CERN; ANID, Chile; CAS, MOST, and NSFC, China;

Minciencias, Colombia; MEYS CR, Czech Republic; DNRf and DNSRC, Denmark; IN2P3-CNRS and CEA-DRF/IRFU, France; SRNSFG, Georgia; BMBF, HGF, and MPG, Germany; GSRI, Greece; RGC and Hong Kong SAR, China; ISF and Benozziyo Center, Israel; INFN, Italy; MEXT and JSPS, Japan; CNRST, Morocco; NWO, Netherlands; RCN, Norway; MNiSW, Poland; FCT, Portugal; MNE/IFA, Romania; MESTD, Serbia; MSSR, Slovakia; ARIS and MVZI, Slovenia; DSI/NRF, South Africa; MICIU/AEI, Spain; SRC and Wallenberg Foundation, Sweden; SERI, SNSF, and Cantons of Bern and Geneva, Switzerland; NSTC, Taipei; TENMAK, Türkiye; STFC/UKRI, United Kingdom; DOE and NSF, U.S. Individual groups and members have received support from BCKDF, CANARIE, CRC, and DRAC, Canada; CERN-CZ, FORTE, and PRIMUS, Czech Republic; COST, ERC, ERDF, Horizon 2020, ICSC-NextGenerationEU, and Marie Skłodowska-Curie Actions, European Union; Investissements d'Avenir Labex, Investissements d'Avenir IDEX, and ANR, France; DFG and AvH Foundation, Germany; Herakleitos, Thales, and Aristeia programs cofinanced by EU-ESF and the Greek NSRF, Greece; BSF-NSF and MINERVA, Israel; Norwegian Financial Mechanism 2014-2021, Norway; NCN and NAWA, Poland; La Caixa Banking Foundation, CERCA Programme Generalitat de Catalunya, and PROMETEO and GenT Programmes Generalitat Valenciana, Spain; Göran Gustafssons Stiftelse, Sweden; The Royal Society and Leverhulme Trust, United Kingdom. In addition, individual members wish to acknowledge support from CERN: European Organization for Nuclear Research (CERN PJAS); Chile: Agencia Nacional de Investigación y Desarrollo (FONDECYT 1190886, FONDECYT 1230812, FONDECYT 1230987); China: Chinese Ministry of Science and Technology (MOST-2023YFA1605700),

National Natural Science Foundation of China (NSFC-12175119, NSFC-12275265, NSFC-12075060); Czech Republic: Czech Science Foundation (GACR—24-11373S), Ministry of Education Youth and Sports (FORTE CZ.02.01.01/00/22_008/0004632), PRIMUS Research Programme (PRIMUS/21/SCI/017); EU: H2020 European Research Council (ERC—101002463); European Union: European Research Council (ERC-948254, ERC-101089007), Horizon 2020 Framework Programme (MUCCA—CHIST-ERA-19-XAI-00), European Union, Future Artificial Intelligence Research (FAIR-NextGenerationEU PE00000013), Italian Center for High Performance Computing, Big Data and Quantum Computing (ICSC, NextGenerationEU); France: Agence Nationale de la Recherche (ANR-20-CE31-0013, ANR-21-CE31-0013, ANR-21-CE31-0022, ANR-22-EDIR-0002), Investissements d’Avenir Labex (ANR-11-LABX-0012); Germany: Baden-Württemberg Stiftung (BW Stiftung-Postdoc Eliteprogramme), Deutsche Forschungsgemeinschaft (DFG—469666862, DFG—CR 312/5-2); Italy: Istituto Nazionale di Fisica Nucleare (ICSC, NextGenerationEU), Ministero dell’Università e della Ricerca (PRIN—20223N7F8K—PNRR M4.C2.1.1); Japan: Japan Society for the Promotion of Science (JSPS KAKENHI JP21H05085, JSPS KAKENHI JP22H01227, JSPS KAKENHI JP22H04944, JSPS KAKENHI JP22KK0227); Netherlands: Netherlands Organisation for Scientific Research (NWO Veni 2020—

VI.Veni.202.179); Norway: Research Council of Norway (RCN-314472); Poland: Ministry of Science and Higher Education (IDUB AGH, POB8, D4 no 9722), Polish National Agency for Academic Exchange (PPN/PPO/2020/1/00002/U/00001), Polish National Science Centre (NCN 2021/42/E/ST2/00350, NCN OPUS nr 2022/47/B/ST2/03059, NCN UMO-2019/34/E/ST2/00393, UMO-2020/37/B/ST2/01043, UMO-2021/40/C/ST2/00187, UMO-2022/47/O/ST2/00148, UMO-2023/49/B/ST2/04085); Slovenia: Slovenian Research Agency (ARIS Grant No. J1-3010); Spain: Generalitat Valenciana (Artemisa, FEDER, IDIFEDER/2018/048), Ministry of Science and Innovation (MCIN, NextGenEU PCI2022-135018-2, MICIN, and FEDER PID2021-125273NB, RYC2019-028510-I, RYC2020-030254-I, RYC2021-031273-I, RYC2022-038164-I), PROMETEO, and GenT Programmes Generalitat Valenciana (CIDEAGENT/2019/023, CIDEAGENT/2019/027); Sweden: Swedish Research Council (Swedish Research Council 2023-04654, VR 2018-00482, VR 2022-03845, VR 2022-04683, VR 2023-03403, VR Grant No. 2021-03651), Knut and Alice Wallenberg Foundation (KAW 2018.0157, KAW 2018.0458, KAW 2019.0447, KAW 2022.0358); Switzerland: Swiss National Science Foundation (SNSF—PCEFP2_194658); United Kingdom: Leverhulme Trust (Leverhulme Trust RPG-2020-004), Royal Society (NIF-R1-231091); U.S.: U.S. Department of Energy (ECA DE-AC02-76SF00515), Neubauer Family Foundation.

-
- [1] L. Susskind, Dynamics of spontaneous symmetry breaking in the Weinberg-Salam theory, *Phys. Rev. D* **20**, 2619 (1979).
- [2] B. A. Dobrescu and C. T. Hill, Electroweak symmetry breaking via a top condensation seesaw mechanism, *Phys. Rev. Lett.* **81**, 2634 (1998).
- [3] C. T. Hill, Topcolor assisted technicolor, *Phys. Lett. B* **345**, 483 (1995).
- [4] N. Arkani-Hamed, A. G. Cohen, E. Katz, and A. E. Nelson, The littlest Higgs, *J. High Energy Phys.* **07** (2002) 034.
- [5] D. B. Kaplan, H. Georgi, and S. Dimopoulos, Composite Higgs scalars, *Phys. Lett.* **136B**, 187 (1984).
- [6] K. Agashe, R. Contino, and A. Pomarol, The minimal composite Higgs model, *Nucl. Phys.* **B719**, 165 (2005).
- [7] S. Chakdar, K. Ghosh, S. Nandi, and S. K. Rai, Collider signatures of mirror fermions in the framework of a left-right mirror model, *Phys. Rev. D* **88**, 095005 (2013).
- [8] F. del Aguila and M. J. Bowick, The possibility of new fermions with $\Delta I = 0$ mass, *Nucl. Phys.* **B224**, 107 (1983).
- [9] J. Aguilar-Saavedra, Identifying top partners at LHC, *J. High Energy Phys.* **11** (2009) 030.
- [10] A. Atre, G. Azealos, M. Carena, T. Han, E. Ozcan, J. Santiago, and G. Unel, Model-independent searches for new quarks at the LHC, *J. High Energy Phys.* **08** (2011) 080.
- [11] J. A. Aguilar-Saavedra, R. Benbrik, S. Heinemeyer, and M. Pérez-Victoria, Handbook of vectorlike quarks: Mixing and single production, *Phys. Rev. D* **88**, 094010 (2013).
- [12] M. Buchkremer, G. Cacciapaglia, A. Deandrea, and L. Panizzi, Model independent framework for searches of top partners, *Nucl. Phys.* **B876**, 376 (2013).
- [13] ATLAS Collaboration, Search for pair-produced heavy quarks decaying to Wq in the two-lepton channel at $\sqrt{s} = 7$ TeV with the ATLAS detector, *Phys. Rev. D* **86**, 012007 (2012).
- [14] Y. Okada and L. Panizzi, LHC signatures of vector-like quarks, *Adv. High Energy Phys.* **2013**, 364936 (2013).
- [15] ATLAS Collaboration, Search for pair production of a new heavy quark that decays into a W boson and a light quark in pp collisions at $\sqrt{s} = 8$ TeV with the ATLAS detector, *Phys. Rev. D* **92**, 112007 (2015).
- [16] CMS Collaboration, Search for vectorlike light-flavor quark partners in proton-proton collisions at $\sqrt{s} = 8$ TeV, *Phys. Rev. D* **97**, 072008 (2018).
- [17] ATLAS Collaboration, Search for heavy vector-like quarks coupling to light quarks in proton-proton collisions at $\sqrt{s} = 7$ TeV with the ATLAS detector, *Phys. Lett. B* **712**, 22 (2012).

- [18] A. Buckley, J. M. Butterworth, L. Corpe, D. Huang, and P. Sun, New sensitivity of current LHC measurements to vector-like quarks, *SciPost Phys.* **9**, 069 (2020).
- [19] ATLAS Collaboration, Search for pair-production of vector-like quarks in pp collision events at $\sqrt{s} = 13$ TeV with at least one leptonically decaying Z boson and a third-generation quark with the ATLAS detector, *Phys. Lett. B* **843**, 138019 (2023).
- [20] ATLAS Collaboration, Search for pair-produced vector-like top and bottom partners in events with large missing transverse momentum in pp collisions with the ATLAS detector, *Eur. Phys. J. C* **83**, 719 (2023).
- [21] ATLAS Collaboration, Search for pair-production of vector-like quarks in lepton + jets final states containing at least one b-tagged jet using the run 2 data from the ATLAS experiment, *Phys. Lett. B* **854**, 138743 (2024).
- [22] CMS Collaboration, Search for vector-like quarks in events with two oppositely charged leptons and jets in proton-proton collisions at $\sqrt{s} = 13$ TeV, *Eur. Phys. J. C* **79**, 364 (2019).
- [23] CMS Collaboration, Search for pair production of vector-like quarks in leptonic final states in proton-proton collisions at $\sqrt{s} = 13$ TeV, *J. High Energy Phys.* **07** (2023) 020.
- [24] ATLAS Collaboration, The ATLAS experiment at the CERN Large Hadron Collider, *J. Instrum.* **3**, S08003 (2008).
- [25] G. Avoni *et al.*, The new LUCID-2 detector for luminosity measurement and monitoring in ATLAS, *J. Instrum.* **13**, P07017 (2018).
- [26] ATLAS Collaboration, Performance of the ATLAS trigger system in 2015, *Eur. Phys. J. C* **77**, 317 (2017).
- [27] ATLAS Collaboration, Software and computing for run 3 of the ATLAS experiment at the LHC, [arXiv:2404.06335](https://arxiv.org/abs/2404.06335).
- [28] ATLAS Collaboration, Luminosity determination in pp collisions at $\sqrt{s} = 13$ TeV using the ATLAS detector at the LHC, *Eur. Phys. J. C* **83**, 982 (2023).
- [29] ATLAS Collaboration, ATLAS data quality operations and performance for 2015–2018 data-taking, *J. Instrum.* **15**, P04003 (2020).
- [30] ATLAS Collaboration, The ATLAS simulation infrastructure, *Eur. Phys. J. C* **70**, 823 (2010).
- [31] S. Agostinelli *et al.* (Geant4 Collaboration), Geant4: A simulation toolkit, *Nucl. Instrum. Methods Phys. Res., Sect. A* **506**, 250 (2003).
- [32] T. Sjöstrand, S. Ask, J. R. Christiansen, R. Corke, N. Desai, P. Ilten, S. Mrenna, S. Prestel, C. O. Rasmussen, and P. Z. Skands, An introduction to PYTHIA 8.2, *Comput. Phys. Commun.* **191**, 159 (2015).
- [33] ATLAS Collaboration, The PYTHIA 8 A3 tune description of ATLAS minimum bias and inelastic measurements incorporating the Donnachie-Landshoff diffractive model, Report No. ATL-PHYS-PUB-2016-017, 2016, <https://cds.cern.ch/record/2206965>.
- [34] J. Alwall, M. Herquet, F. Maltoni, O. Mattelaer, and T. Stelzer, MadGraph 5: Going beyond, *J. High Energy Phys.* **06** (2011) 128.
- [35] R. D. Ball *et al.* (NNPDF Collaboration), Parton distributions for the LHC run II, *J. High Energy Phys.* **04** (2015) 040.
- [36] M. Czakon and A. Mitov, Top++: A program for the calculation of the top-pair cross-section at hadron colliders, *Comput. Phys. Commun.* **185**, 2930 (2014).
- [37] E. Bothmann *et al.*, Event generation with Sherpa 2.2, *SciPost Phys.* **7**, 034 (2019).
- [38] T. Gleisberg and S. Höche, Comix, a new matrix element generator, *J. High Energy Phys.* **12** (2008) 039.
- [39] F. Buccioni, J.-N. Lang, J. M. Lindert, P. Maierhöfer, S. Pozzorini, H. Zhang, and M. F. Zoller, OpenLoops 2, *Eur. Phys. J. C* **79**, 866 (2019).
- [40] F. Cascioli, P. Maierhofer, and S. Pozzorini, Scattering amplitudes with OpenLoops, *Phys. Rev. Lett.* **108**, 111601 (2012).
- [41] A. Denner, S. Dittmaier, and L. Hofer, Collier: A Fortran-based complex one-loop library in extended regularizations, *Comput. Phys. Commun.* **212**, 220 (2017).
- [42] S. Schumann and F. Krauss, A parton shower algorithm based on Catani-Seymour dipole factorisation, *J. High Energy Phys.* **03** (2008) 038.
- [43] S. Höche, F. Krauss, M. Schönherr, and F. Siegert, A critical appraisal of NLO + PS matching methods, *J. High Energy Phys.* **09** (2012) 049.
- [44] S. Höche, F. Krauss, M. Schönherr, and F. Siegert, QCD matrix elements + parton showers: The NLO case, *J. High Energy Phys.* **04** (2013) 027.
- [45] S. Catani, F. Krauss, B. R. Webber, and R. Kuhn, QCD matrix elements + parton showers, *J. High Energy Phys.* **11** (2001) 063.
- [46] S. Höche, F. Krauss, S. Schumann, and F. Siegert, QCD matrix elements and truncated showers, *J. High Energy Phys.* **05** (2009) 053.
- [47] C. Anastasiou, L. J. Dixon, K. Melnikov, and F. Petriello, High precision QCD at hadron colliders: Electroweak gauge boson rapidity distributions at NNLO, *Phys. Rev. D* **69**, 094008 (2004).
- [48] S. Frixione, P. Nason, and G. Ridolfi, A positive-weight next-to-leading-order Monte Carlo for heavy flavour hadroproduction, *J. High Energy Phys.* **09** (2007) 126.
- [49] P. Nason, A new method for combining NLO QCD with shower Monte Carlo algorithms, *J. High Energy Phys.* **11** (2004) 040.
- [50] S. Frixione, P. Nason, and C. Oleari, Matching NLO QCD computations with parton shower simulations: The POWHEG method, *J. High Energy Phys.* **11** (2007) 070.
- [51] S. Alioli, P. Nason, C. Oleari, and E. Re, A general framework for implementing NLO calculations in shower Monte Carlo programs: The POWHEG BOX, *J. High Energy Phys.* **06** (2010) 043.
- [52] ATLAS Collaboration, Studies on top-quark Monte Carlo modelling for Top2016, Report No. ATL-PHYS-PUB-2016-020, 2016, <https://cds.cern.ch/record/2216168>.
- [53] ATLAS Collaboration, ATLAS PYTHIA 8 tunes to 7 TeV data, Report No. ATL-PHYS-PUB-2014-021, 2014, <https://cds.cern.ch/record/1966419>.
- [54] R. D. Ball *et al.* (NNPDF Collaboration), Parton distributions with LHC data, *Nucl. Phys.* **B867**, 244 (2013).
- [55] M. Bahr *et al.*, Herwig++ physics and manual, *Eur. Phys. J. C* **58**, 639 (2008).
- [56] J. Bellm *et al.*, Herwig 7.0/Herwig++ 3.0 release note, *Eur. Phys. J. C* **76**, 196 (2016).
- [57] L. A. Harland-Lang, A. D. Martin, P. Motylinski, and R. S. Thorne, Parton distributions in the LHC era: MMHT 2014 PDFs, *Eur. Phys. J. C* **75**, 204 (2015).

- [58] J. Alwall, R. Frederix, S. Frixione, V. Hirschi, F. Maltoni, O. Mattelaer, H.-S. Shao, T. Stelzer, P. Torrielli, and M. Zaro, The automated computation of tree-level and next-to-leading order differential cross sections, and their matching to parton shower simulations, *J. High Energy Phys.* **07** (2014) 079.
- [59] E. Re, Single-top Wt -channel production matched with parton showers using the POWHEG method, *Eur. Phys. J. C* **71**, 1547 (2011).
- [60] S. Frixione, E. Laenen, P. Motylinski, B. R. Webber, and C. D. White, Single-top hadroproduction in association with a W boson, *J. High Energy Phys.* **07** (2008) 029.
- [61] H.-L. Lai, M. Guzzi, J. Huston, Z. Li, P. M. Nadolsky, J. Pumplin, and C.-P. Yuan, New parton distributions for collider physics, *Phys. Rev. D* **82**, 074024 (2010).
- [62] ATLAS Collaboration, Electron and photon performance measurements with the ATLAS detector using the 2015–2017 LHC proton-proton collision data, *J. Instrum.* **14**, P12006 (2019).
- [63] ATLAS Collaboration, Muon reconstruction and identification efficiency in ATLAS using the full run $2pp$ collision data set at $\sqrt{s} = 13$ TeV, *Eur. Phys. J. C* **81**, 578 (2021).
- [64] ATLAS Collaboration, Jet reconstruction and performance using particle flow with the ATLAS Detector, *Eur. Phys. J. C* **77**, 466 (2017).
- [65] M. Cacciari, G. P. Salam, and G. Soyez, The anti- k_r jet clustering algorithm, *J. High Energy Phys.* **04** (2008) 063.
- [66] M. Cacciari, G. P. Salam, and G. Soyez, FastJet user manual, *Eur. Phys. J. C* **72**, 1896 (2012).
- [67] ATLAS Collaboration, Jet energy scale and resolution measured in proton-proton collisions at $\sqrt{s} = 13$ TeV with the ATLAS detector, *Eur. Phys. J. C* **81**, 689 (2021).
- [68] ATLAS Collaboration, Performance of pile-up mitigation techniques for jets in pp collisions at $\sqrt{s} = 8$ TeV using the ATLAS detector, *Eur. Phys. J. C* **76**, 581 (2016).
- [69] ATLAS Collaboration, ATLAS flavour-tagging algorithms for the LHC run $2pp$ collision dataset, *Eur. Phys. J. C* **83**, 681 (2023).
- [70] ATLAS Collaboration, ATLAS b -jet identification performance and efficiency measurement with $t\bar{t}$ events in pp collisions at $\sqrt{s} = 13$ TeV, *Eur. Phys. J. C* **79**, 970 (2019).
- [71] ATLAS Collaboration, Measurement of the c -jet mistagging efficiency in $t\bar{t}$ events using pp collision data at $\sqrt{s} = 13$ TeV collected with the ATLAS detector, *Eur. Phys. J. C* **82**, 95 (2022).
- [72] ATLAS Collaboration, Calibration of the light-flavour jet mistagging efficiency of the b -tagging algorithms with $Z +$ jets events using 139 fb^{-1} of ATLAS proton-proton collision data at $\sqrt{s} = 13$ TeV, *Eur. Phys. J. C* **83**, 728 (2023).
- [73] ATLAS Collaboration, Topological cell clustering in the ATLAS calorimeters and its performance in LHC run 1, *Eur. Phys. J. C* **77**, 490 (2017).
- [74] ATLAS Collaboration, Performance of top-quark and W -boson tagging with ATLAS in run 2 of the LHC, *Eur. Phys. J. C* **79**, 375 (2019).
- [75] A. J. Larkoski, I. Moulton, and D. Neill, Power counting to better jet observables, *J. High Energy Phys.* **12** (2014) 009.
- [76] ATLAS Collaboration, Boosted hadronic vector boson and top quark tagging with ATLAS using run 2 data, Report No. ATL-PHYS-PUB-2020-017, 2020, <https://cds.cern.ch/record/2724149>.
- [77] ATLAS Collaboration, The performance of missing transverse momentum reconstruction and its significance with the ATLAS detector using 140 fb^{-1} of $\sqrt{s} = 13$ TeV pp collisions, [arXiv:2402.05858](https://arxiv.org/abs/2402.05858).
- [78] ATLAS Collaboration, Performance of electron and photon triggers in ATLAS during LHC run 2, *Eur. Phys. J. C* **80**, 47 (2020).
- [79] ATLAS Collaboration, Performance of the ATLAS muon triggers in run 2, *J. Instrum.* **15**, P09015 (2020).
- [80] R. L. Workman *et al.* (Particle Data Group), Review of particle physics, *Prog. Theor. Exp. Phys.* **2022**, 083C01 (2022).
- [81] ATLAS Collaboration, ATLAS simulation of boson plus jets processes in run 2, Report No. ATL-PHYS-PUB-2017-006, 2017, <https://cds.cern.ch/record/2261937>.
- [82] ATLAS Collaboration, Studies of the muon momentum calibration and performance of the ATLAS detector with pp collisions at $\sqrt{s} = 13$ TeV, *Eur. Phys. J. C* **83**, 686 (2023).
- [83] ATLAS Collaboration, In situ calibration of large-radius jet energy and mass in 13 TeV proton-proton collisions with the ATLAS detector, *Eur. Phys. J. C* **79**, 135 (2019).
- [84] ATLAS Collaboration, Measurement of the ATLAS detector jet mass response using forward folding with 80 fb^{-1} of $\sqrt{s} = 13$ TeV pp data, Report No. ATLAS-CONF-2020-022, 2020, <https://cds.cern.ch/record/2724442>.
- [85] J. Butterworth *et al.*, PDF4LHC recommendations for LHC run II, *J. Phys. G* **43**, 023001 (2016).
- [86] ATLAS Collaboration, Studies of $t\bar{t}/tW$ interference effects in $b\bar{b}e^+e^-\nu\bar{\nu}'$ final states with POWHEG and MadGraph5_aMC@NLO setups, Report No. ATL-PHYS-PUB-2021-042, 2021, <https://cds.cern.ch/record/2792254>.
- [87] ATLAS Collaboration, ATLAS computing acknowledgements, Report No. ATL-SOFT-PUB-2023-001, 2023, <https://cds.cern.ch/record/2869272>.

G. Aad¹⁰⁴, E. Aakvaag¹⁷, B. Abbott¹²³, S. Abdelhameed^{119a}, K. Abeling⁵⁶, N. J. Abicht⁵⁰, S. H. Abidi³⁰, M. Aboelela⁴⁵, A. Aboulhorma^{36e}, H. Abramowicz¹⁵⁴, H. Abreu¹⁵³, Y. Abulaiti¹²⁰, B. S. Acharya^{70a,70b,b}, A. Ackermann^{64a}, C. Adam Bourdarios⁴, L. Adamczyk^{87a}, S. V. Addepalli²⁷, M. J. Addison¹⁰³, J. Adelman¹¹⁸, A. Adiguzel^{22c}, T. Adye¹³⁷, A. A. Affolder¹³⁹, Y. Afik⁴⁰, M. N. Agaras¹³, J. Agarwala^{74a,74b}, A. Aggarwal¹⁰², C. Agheorghiesei^{28c}, F. Ahmadov^{39,c}, W. S. Ahmed¹⁰⁶, S. Ahuja⁹⁷, X. Ai^{63e}, G. Aielli^{77a,77b}, A. Aikot¹⁶⁶, M. Ait Tamlihat^{36e}, B. Aitbenchikh^{36a}, M. Akbiyik¹⁰², T. P. A. Åkesson¹⁰⁰, A. V. Akimov³⁸, D. Akiyama¹⁷¹

N. N. Akolkar²⁵ S. Aktas^{22a} K. Al Houry⁴² G. L. Alberghi^{24b} J. Albert¹⁶⁸ P. Albicocco⁵⁴ G. L. Albouy⁶¹
 S. Alderweireldt⁵³ Z. L. Alegria¹²⁴ M. Aleksa³⁷ I. N. Aleksandrov³⁹ C. Alexa^{28b} T. Alexopoulos¹⁰
 F. Alfonsi^{24b} M. Algren⁵⁷ M. Alhroob¹⁷⁰ B. Ali¹³⁵ H. M. J. Ali⁹³ S. Ali³² S. W. Alibocus⁹⁴ M. Aliev^{34c}
 G. Alimonti^{72a} W. Alkahi⁵⁶ C. Allaire⁶⁷ B. M. M. Allbrooke¹⁴⁹ J. F. Allen⁵³ C. A. Allendes Flores^{140f}
 P. P. Allport²¹ A. Aloisio^{73a,73b} F. Alonso⁹² C. Alpigiani¹⁴¹ Z. M. K. Alsolami⁹³ M. Alvarez Estevez¹⁰¹
 A. Alvarez Fernandez¹⁰² M. Alves Cardoso⁵⁷ M. G. Alviggi^{73a,73b} M. Aly¹⁰³ Y. Amaral Coutinho^{84b}
 A. Ambler¹⁰⁶ C. Amelung³⁷ M. Amerl¹⁰³ C. G. Ames¹¹¹ D. Amidei¹⁰⁸ K. J. Amirie¹⁵⁸
 S. P. Amor Dos Santos^{133a} K. R. Amos¹⁶⁶ S. An⁸⁵ V. Ananiev¹²⁸ C. Anastopoulos¹⁴² T. Andeen¹¹
 J. K. Anders³⁷ A. C. Anderson⁶⁰ S. Y. Andreato^{48a,48b} A. Andreazza^{72a,72b} S. Angelidakis⁹ A. Angerami⁴²
 A. V. Anisenkov³⁸ A. Annovi^{75a} C. Antelov⁵⁷ E. Antipov¹⁴⁸ M. Antonelli⁵⁴ F. Anulli^{76a} M. Aoki⁸⁵
 T. Aoki¹⁵⁶ M. A. Aparo¹⁴⁹ L. Aperio Bella⁴⁹ C. Appelt¹⁹ A. Apyan²⁷ S. J. Arbiol Val⁸⁸ C. Arcangeletti⁵⁴
 A. T. H. Arce⁵² E. Arena⁹⁴ J-F. Arguin¹¹⁰ S. Argyropoulos⁵⁵ J.-H. Arling⁴⁹ O. Arnaez⁴ H. Arnold¹⁴⁸
 G. Artoni^{76a,76b} H. Asada¹¹³ K. Asai¹²¹ S. Asai¹⁵⁶ N. A. Asbah³⁷ R. A. Ashby Pickering¹⁷⁰ K. Assamagan³⁰
 R. Astalos^{29a} K. S. V. Astrand¹⁰⁰ S. Atashi¹⁶² R. J. Atkin^{34a} M. Atkinson¹⁶⁵ H. Atmani^{36f} P. A. Atmasiddha¹³¹
 K. Augsten¹³⁵ S. Auricchio^{73a,73b} A. D. Auriol²¹ V. A. Austrup¹⁰³ G. Avolio³⁷ K. Axiotis⁵⁷ G. Azuelos^{110,d}
 D. Babal^{29b} H. Bachacou¹³⁸ K. Bachas^{155,e} A. Bachi³⁵ F. Backman^{48a,48b} A. Badea⁴⁰ T. M. Baer¹⁰⁸
 P. Bagnaia^{76a,76b} M. Bahmani¹⁹ D. Bahner⁵⁵ K. Bai¹²⁶ J. T. Baines¹³⁷ L. Baines⁹⁶ O. K. Baker¹⁷⁵
 E. Bakos¹⁶ D. Bakshi Gupta⁸ L. E. Balabram Filho^{84b} V. Balakrishnan¹²³ R. Balasubramanian¹¹⁷
 E. M. Baldin³⁸ P. Balek^{87a} E. Ballabene^{24b,24a} F. Balli¹³⁸ L. M. Baltes^{64a} W. K. Balunas³³ J. Balz¹⁰²
 I. Bamwidhi^{119b} E. Banas⁸⁸ M. Bandieramonte¹³² A. Bandyopadhyay²⁵ S. Bansal²⁵ L. Barak¹⁵⁴
 M. Barakat⁴⁹ E. L. Barberio¹⁰⁷ D. Barberis^{58b,58a} M. Barbero¹⁰⁴ M. Z. Barel¹¹⁷ K. N. Barends^{34a}
 T. Barillari¹¹² M-S. Barisits³⁷ T. Barklow¹⁴⁶ P. Baron¹²⁵ D. A. Baron Moreno¹⁰³ A. Baroncelli^{63a}
 A. J. Barr¹²⁹ J. D. Barr⁹⁸ F. Barreiro¹⁰¹ J. Barreiro Guimarães da Costa¹⁴ U. Barron¹⁵⁴
 M. G. Barros Teixeira^{133a} S. Barsov³⁸ F. Bartels^{64a} R. Bartoldus¹⁴⁶ A. E. Barton⁹³ P. Bartos^{29a} A. Basan¹⁰²
 M. Baselga⁵⁰ A. Bassalat^{67,f} M. J. Basso^{159a} S. Bataju⁴⁵ R. Bate¹⁶⁷ R. L. Bates⁶⁰ S. Batlamous¹⁰¹
 B. Batool¹⁴⁴ M. Battaglia¹³⁹ D. Battulga¹⁹ M. Bauce^{76a,76b} M. Bauer⁸⁰ P. Bauer²⁵ L. T. Bazzano Hurrell³¹
 J. B. Beacham⁵² T. Beau¹³⁰ J. Y. Beaucamp⁹² P. H. Beauchemin¹⁶¹ P. Bechtel²⁵ H. P. Beck^{20,g} K. Becker¹⁷⁰
 A. J. Beddall⁸³ V. A. Bednyakov³⁹ C. P. Bee¹⁴⁸ L. J. Beemster¹⁶ T. A. Beermann³⁷ M. Begalli^{84d} M. Begel³⁰
 A. Behera¹⁴⁸ J. K. Behr⁴⁹ J. F. Beirer³⁷ F. Beisiegel²⁵ M. Belfkir^{119b} G. Bella¹⁵⁴ L. Bellagamba^{24b}
 A. Bellerive³⁵ P. Bellos²¹ K. Beloborodov³⁸ D. Benckekroun^{36a} F. Bendebba^{36a} Y. Benhammou¹⁵⁴
 K. C. Benkendorfer⁶² L. Beresford⁴⁹ M. Beretta⁵⁴ E. Bergeas Kuutmann¹⁶⁴ N. Berger⁴ B. Bergmann¹³⁵
 J. Beringer^{18a} G. Bernardi⁵ C. Bernius¹⁴⁶ F. U. Bernlochner²⁵ F. Bernon^{37,104} A. Berrocal Guardia¹³
 T. Berry⁹⁷ P. Berta¹³⁶ A. Berthold⁵¹ S. Bethke¹¹² A. Betti^{76a,76b} A. J. Bevan⁹⁶ N. K. Bhalla⁵⁵ S. Bhatta¹⁴⁸
 D. S. Bhattacharya¹⁶⁹ P. Bhattarai¹⁴⁶ K. D. Bhide⁵⁵ V. S. Bhopatkar¹²⁴ R. M. Bianchi¹³² G. Bianco^{24b,24a}
 O. Biebel¹¹¹ R. Bielski¹²⁶ M. Biglietti^{78a} C. S. Billingsley⁴⁵ M. Bindi⁵⁶ A. Bingul^{22b} C. Bini^{76a,76b}
 A. Biondini⁹⁴ G. A. Bird³³ M. Birman¹⁷² M. Biros¹³⁶ S. Biryukov¹⁴⁹ T. Bisanz⁵⁰ E. Bisceglie^{44b,44a}
 J. P. Biswal¹³⁷ D. Biswas¹⁴⁴ I. Bloch⁴⁹ A. Blue⁶⁰ U. Blumenschein⁹⁶ J. Blumenthal¹⁰² V. S. Bobrovnikov³⁸
 M. Boehler⁵⁵ B. Boehm¹⁶⁹ D. Bogavac³⁷ A. G. Bogdanchikov³⁸ C. Bohm^{48a} V. Boisvert⁹⁷ P. Bokan³⁷
 T. Bold^{87a} M. Bomben⁵ M. Bona⁹⁶ M. Boonekamp¹³⁸ C. D. Booth⁹⁷ A. G. Borbély⁶⁰ I. S. Bordulev³⁸
 H. M. Borecka-Bielska¹¹⁰ G. Borissov⁹³ D. Bortoletto¹²⁹ D. Boscherini^{24b} M. Bosman¹³ J. D. Bossio Sola³⁷
 K. Bouaouda^{36a} N. Bouchhar¹⁶⁶ L. Boudet⁴ J. Boudreau¹³² E. V. Bouhova-Thacker⁹³ D. Boumediene⁴¹
 R. Bouquet^{58b,58a} A. Boveia¹²² J. Boyd³⁷ D. Boye³⁰ I. R. Boyko³⁹ L. Bozianu⁵⁷ J. Bracinik²¹ N. Brahimi⁴
 G. Brandt¹⁷⁴ O. Brandt³³ F. Braren⁴⁹ B. Brau¹⁰⁵ J. E. Brau¹²⁶ R. Brenner¹⁷² L. Brenner¹¹⁷ R. Brenner¹⁶⁴
 S. Bressler¹⁷² G. Brianti^{79a,79b} D. Britton⁶⁰ D. Britzger¹¹² I. Brock²⁵ G. Brooijmans⁴² E. M. Brooks^{159b}
 E. Brost³⁰ L. M. Brown¹⁶⁸ L. E. Bruce⁶² T. L. Bruckler¹²⁹ P. A. Bruckman de Renstrom⁸⁸ B. Brüers⁴⁹
 A. Bruni^{24b} G. Bruni^{24b} M. Bruschi^{24b} N. Bruscino^{76a,76b} T. Buanes¹⁷ Q. Buat¹⁴¹ D. Buchin¹¹²
 A. G. Buckley⁶⁰ O. Bulekov³⁸ B. A. Bullard¹⁴⁶ S. Burdin⁹⁴ C. D. Burgard⁵⁰ A. M. Burger³⁷ B. Burghgrave⁸
 O. Burlayenko⁵⁵ J. Burlinson¹⁶⁵ J. T. P. Burr³³ J. C. Burzynski¹⁴⁵ E. L. Busch⁴² V. Büscher¹⁰² P. J. Bussey⁶⁰
 J. M. Butler²⁶ C. M. Buttar⁶⁰ J. M. Butterworth⁹⁸ W. Buttinger¹³⁷ C. J. Buxo Vazquez¹⁰⁹ A. R. Buzykaev³⁸

S. Cabrera Urbán¹⁶⁶ L. Cadamuro⁶⁷ D. Caforio⁵⁹ H. Cai¹³² Y. Cai^{14,114c} Y. Cai^{114a} V. M. M. Cairo³⁷
O. Cakir^{3a} N. Calace³⁷ P. Calafiura^{18a} G. Calderini¹³⁰ P. Calfayan⁶⁹ G. Callea⁶⁰ L. P. Caloba^{84b} D. Calvet⁴¹
S. Calvet⁴¹ M. Calvetti^{75a,75b} R. Camacho Toro¹³⁰ S. Camarda³⁷ D. Camarero Munoz²⁷ P. Camarri^{77a,77b}
M. T. Camerlingo^{73a,73b} D. Cameron³⁷ C. Camincher¹⁶⁸ M. Campanelli⁹⁸ A. Camplani⁴³ V. Canale^{73a,73b}
A. C. Canbay^{3a} E. Canonero⁹⁷ J. Cantero¹⁶⁶ Y. Cao¹⁶⁵ F. Capocasa²⁷ M. Capua^{44b,44a} A. Carbone^{72a,72b}
R. Cardarelli^{77a} J. C. J. Cardenas⁸ G. Carducci^{44b,44a} T. Carli³⁷ G. Carlino^{73a} J. I. Carlotto¹³
B. T. Carlson^{132,h} E. M. Carlson^{168,159a} J. Carmignani⁹⁴ L. Carminati^{72a,72b} A. Carnelli¹³⁸ M. Carnesale^{76a,76b}
S. Caron¹¹⁶ E. Carquin^{140f} S. Carrá^{72a} G. Carratta^{24b,24a} A. M. Carroll¹²⁶ T. M. Carter⁵³ M. P. Casado^{13,i}
M. Caspar⁴⁹ F. L. Castillo⁴ L. Castillo Garcia¹³ V. Castillo Gimenez¹⁶⁶ N. F. Castro^{133a,133e} A. Catinaccio³⁷
J. R. Catmore¹²⁸ T. Cavaliere⁴ V. Cavaliere³⁰ N. Cavalli^{24b,24a} L. J. Caviedes Betancourt^{23b}
Y. C. Cekmecelioglu⁴⁹ E. Celebi⁸³ S. Cella³⁷ F. Celli¹²⁹ M. S. Centonze^{71a,71b} V. Cepaitis⁵⁷ K. Cerny¹²⁵
A. S. Cerqueira^{84a} A. Cerri¹⁴⁹ L. Cerrito^{77a,77b} F. Cerutti^{18a} B. Cervato¹⁴⁴ A. Cervelli^{24b} G. Cesarini⁵⁴
S. A. Cetin⁸³ D. Chakraborty¹¹⁸ J. Chan^{18a} W. Y. Chan¹⁵⁶ J. D. Chapman³³ E. Chapon¹³⁸
B. Chargeishvili^{152b} D. G. Charlton²¹ M. Chatterjee²⁰ C. Chauhan¹³⁶ Y. Che^{114a} S. Chekanov⁶
S. V. Chekulaev^{159a} G. A. Chelkov^{39,j} A. Chen¹⁰⁸ B. Chen¹⁵⁴ B. Chen¹⁶⁸ H. Chen^{114a} H. Chen³⁰
J. Chen^{63c} J. Chen¹⁴⁵ M. Chen¹²⁹ S. Chen¹⁵⁶ S. J. Chen^{114a} X. Chen^{63c,138} X. Chen^{15,k} Y. Chen^{63a}
C. L. Cheng¹⁷³ H. C. Cheng^{65a} S. Cheong¹⁴⁶ A. Cheplakov³⁹ E. Cheremushkina⁴⁹ E. Cherepanova¹¹⁷
R. Cherkaoui El Moursli^{36e} E. Cheu⁷ K. Cheung⁶⁶ L. Chevalier¹³⁸ V. Chiarella⁵⁴ G. Chiarelli^{75a}
N. Chiedde¹⁰⁴ G. Chiodini^{71a} A. S. Chisholm²¹ A. Chitan^{28b} M. Chitishvili¹⁶⁶ M. V. Chizhov^{39,l} K. Choi¹¹
Y. Chou¹⁴¹ E. Y. S. Chow¹¹⁶ K. L. Chu¹⁷² M. C. Chu^{65a} X. Chu^{14,114c} Z. Chubinidze⁵⁴ J. Chudoba¹³⁴
J. J. Chwastowski⁸⁸ D. Cieri¹¹² K. M. Ciesla^{87a} V. Cindro⁹⁵ A. Ciocio^{18a} F. Ciroto^{73a,73b} Z. H. Citron¹⁷²
M. Citterio^{72a} D. A. Ciubotaru^{28b} A. Clark⁵⁷ P. J. Clark⁵³ N. Clarke Hall⁹⁸ C. Clarry¹⁵⁸
J. M. Clavijo Columbie⁴⁹ S. E. Clawson⁴⁹ C. Clement^{48a,48b} Y. Coadou¹⁰⁴ M. Cobal^{70a,70c} A. Coccaro^{58b}
R. F. Coelho Barrue^{133a} R. Coelho Lopes De Sa¹⁰⁵ S. Coelli^{72a} B. Cole⁴² J. Collot⁶¹ P. Conde Muino^{133a,133g}
M. P. Connell^{34c} S. H. Connell^{34c} E. I. Conroy¹²⁹ F. Conventi^{73a,m} H. G. Cooke²¹ A. M. Cooper-Sarkar¹²⁹
F. A. Corchia^{24b,24a} A. Cordeiro Oudot Choi¹³⁰ L. D. Corpe⁴¹ M. Corradi^{76a,76b} F. Corriveau^{106,n}
A. Cortes-Gonzalez¹⁹ M. J. Costa¹⁶⁶ F. Costanza⁴ D. Costanzo¹⁴² B. M. Cote¹²² J. Couthures⁴ G. Cowan⁹⁷
K. Cranmer¹⁷³ D. Cremonini^{24b,24a} S. Crépe-Renaudin⁶¹ F. Crescioli¹³⁰ M. Cristinziani¹⁴⁴
M. Cristoforetti^{79a,79b} V. Croft¹¹⁷ J. E. Crosby¹²⁴ G. Crosetti^{44b,44a} A. Cueto¹⁰¹ H. Cui⁹⁸ Z. Cui⁷
W. R. Cunningham⁶⁰ F. Curcio¹⁶⁶ J. R. Curran⁵³ P. Czodrowski³⁷ M. M. Czurylo³⁷
M. J. Da Cunha Sargedas De Sousa^{58b,58a} J. V. Da Fonseca Pinto^{84b} C. Da Via¹⁰³ W. Dabrowski^{87a} T. Dado⁵⁰
S. Dahbi¹⁵¹ T. Dai¹⁰⁸ D. Dal Santo²⁰ C. Dallapiccola¹⁰⁵ M. Dam⁴³ G. D'amen³⁰ V. D'Amico¹¹¹
J. Damp¹⁰² J. R. Dandoy³⁵ D. Dannheim³⁷ M. Danninger¹⁴⁵ V. Dao¹⁴⁸ G. Darbo^{58b} S. J. Das^{30,o}
F. Dattola⁴⁹ S. D'Auria^{72a,72b} A. D'Avanzo^{73a,73b} C. David^{34a} T. Davidek¹³⁶ I. Dawson⁹⁶ H. A. Day-hall¹³⁵
K. De⁸ R. De Asmundis^{73a} N. De Biase⁴⁹ S. De Castro^{24b,24a} N. De Groot¹¹⁶ P. de Jong¹¹⁷ H. De la Torre¹¹⁸
A. De Maria^{114a} A. De Salvo^{76a} U. De Sanctis^{77a,77b} F. De Santis^{71a,71b} A. De Santo¹⁴⁹
J. B. De Vivie De Regie⁶¹ D. V. Dedovich³⁹ J. Degen⁹⁴ A. M. Deiana⁴⁵ F. Del Corso^{24b,24a} J. Del Peso¹⁰¹
F. Del Rio^{64a} L. Delagrangé¹³⁰ F. Deliot¹³⁸ C. M. Delitzsch⁵⁰ M. Della Pietra^{73a,73b} D. Della Volpe⁵⁷
A. Dell'Acqua³⁷ L. Dell'Asta^{72a,72b} M. Delmastro⁴ P. A. Delsart⁶¹ S. Demers¹⁷⁵ M. Demichev³⁹
S. P. Denisov³⁸ L. D'Eramo⁴¹ D. Derendarz⁸⁸ F. Derue¹³⁰ P. Dervan⁹⁴ K. Desch²⁵ C. Deutsch²⁵
F. A. Di Bello^{58b,58a} A. Di Ciaccio^{77a,77b} L. Di Ciaccio⁴ A. Di Domenico^{76a,76b} C. Di Donato^{73a,73b}
A. Di Girolamo³⁷ G. Di Gregorio³⁷ A. Di Luca^{79a,79b} B. Di Micco^{78a,78b} R. Di Nardo^{78a,78b} K. F. Di Petrillo⁴⁰
M. Diamantopoulou³⁵ F. A. Dias¹¹⁷ T. Dias Do Vale¹⁴⁵ M. A. Diaz^{140a,140b} F. G. Diaz Capriles²⁵
A. R. Didenko³⁹ M. Didenko¹⁶⁶ E. B. Diehl¹⁰⁸ S. Díez Cornell⁴⁹ C. Díez Pardos¹⁴⁴ C. Dimitriadi¹⁶⁴
A. Dimitrievska²¹ J. Dingfelder²⁵ T. Dingley¹²⁹ I-M. Dinu^{28b} S. J. Dittmeier^{64b} F. Dittus³⁷ M. Divisek¹³⁶
F. Djama¹⁰⁴ T. Djobava^{152b} C. Doglioni^{103,100} A. Dohnalova^{29a} J. Dolejsi¹³⁶ Z. Dolezal¹³⁶ K. Domijan^{87a}
K. M. Dona⁴⁰ M. Donadelli^{84d} B. Dong¹⁰⁹ J. Donini⁴¹ A. D'Onofrio^{73a,73b} M. D'Onofrio⁹⁴ J. Dopke¹³⁷
A. Doria^{73a} N. Dos Santos Fernandes^{133a} P. Dougan¹⁰³ M. T. Dova⁹² A. T. Doyle⁶⁰ M. A. Dragnet¹²⁹
E. Dreyer¹⁷² I. Drivas-koulouris¹⁰ M. Drnevich¹²⁰ M. Drozdova⁵⁷ D. Du^{63a} T. A. du Pree¹¹⁷ F. Dubinin³⁸

M. Dubovsky^{29a} E. Duchovni¹⁷² G. Duckeck¹¹¹ O. A. Ducu^{28b} D. Duda⁵³ A. Dudarev³⁷ E. R. Duden²⁷
M. D'uffizi¹⁰³ L. Dufлот⁶⁷ M. Dürrssen³⁷ I. Duminica^{28g} A. E. Dumitriu^{28b} M. Dunford^{64a} S. Dungs⁵⁰
K. Dunne^{48a,48b} A. Duperrin¹⁰⁴ H. Duran Yildiz^{3a} M. Düren⁵⁹ A. Durglishvili^{152b} B. L. Dwyer¹¹⁸
G. I. Dyckes^{18a} M. Dyndal^{87a} B. S. Dziedzic³⁷ Z. O. Earnshaw¹⁴⁹ G. H. Eberwein¹²⁹ B. Eckerova^{29a}
S. Eggebrecht⁵⁶ E. Egidio Purcino De Souza¹³⁰ L. F. Ehrke⁵⁷ G. Eigen¹⁷ K. Einsweiler^{18a} T. Ekelof¹⁶⁴
P. A. Ekman¹⁰⁰ S. El Farkh^{36b} Y. El Ghazali^{36b} H. El Jarrari³⁷ A. El Moussaouy^{36a} V. Ellajosyula¹⁶⁴
M. Ellert¹⁶⁴ F. Ellinghaus¹⁷⁴ N. Ellis³⁷ J. Elmsheuser³⁰ M. Elsayw^{119a} M. Elsing³⁷ D. Emelianov¹³⁷
Y. Enari¹⁵⁶ I. Ene^{18a} S. Epari¹³ P. A. Erland⁸⁸ D. Ernani Martins Neto⁸⁸ M. Errenst¹⁷⁴ M. Escalier⁶⁷
C. Escobar¹⁶⁶ E. Etzion¹⁵⁴ G. Evans^{133a} H. Evans⁶⁹ L. S. Evans⁹⁷ A. Ezhilov³⁸ S. Ezzarqtouni^{36a}
F. Fabbri^{24b,24a} L. Fabbri^{24b,24a} G. Facini⁹⁸ V. Fadeyev¹³⁹ R. M. Fakhruddinov³⁸ D. Fakoudis¹⁰²
S. Falciano^{76a} L. F. Falda Ulhoa Coelho³⁷ F. Fallavollita¹¹² G. Falsetti^{44b,44a} J. Faltova¹³⁶ C. Fan¹⁶⁵ Y. Fan¹⁴
Y. Fang^{14,114c} M. Fanti^{72a,72b} M. Faraj^{70a,70b} Z. Farazpay⁹⁹ A. Farbin⁸ A. Farilla^{78a} T. Farooque¹⁰⁹
S. M. Farrington⁵³ F. Fassi^{36e} D. Fassouliotis⁹ M. Faucci Giannelli^{77a,77b} W. J. Fawcett³³ L. Fayard⁶⁷
P. Federic¹³⁶ P. Federicova¹³⁴ O. L. Fedin^{38j} M. Feickert¹⁷³ L. Feligioni¹⁰⁴ D. E. Fellers¹²⁶ C. Feng^{63b}
M. Feng¹⁵ Z. Feng¹¹⁷ M. J. Fenton¹⁶² L. Ferencz⁴⁹ R. A. M. Ferguson⁹³ S. I. Fernandez Luengo^{140f}
P. Fernandez Martinez¹³ M. J. V. Fernoux¹⁰⁴ J. Ferrando⁹³ A. Ferrari¹⁶⁴ P. Ferrari^{117,116} R. Ferrari^{74a}
D. Ferrere⁵⁷ C. Ferretti¹⁰⁸ D. Fiacco^{76a,76b} F. Fiedler¹⁰² P. Fiedler¹³⁵ A. Filipčić⁹⁵ E. K. Filmer¹
F. Filthaut¹¹⁶ M. C. N. Fiolhais^{133a,133c,p} L. Fiorini¹⁶⁶ W. C. Fisher¹⁰⁹ T. Fitschen¹⁰³ P. M. Fitzhugh¹³⁸
I. Fleck¹⁴⁴ P. Fleischmann¹⁰⁸ T. Flick¹⁷⁴ M. Flores^{34d,q} L. R. Flores Castillo^{65a} L. Flores Sanz De Acedo³⁷
F. M. Follega^{79a,79b} N. Fomin³³ J. H. Foo¹⁵⁸ A. Formica¹³⁸ A. C. Forti¹⁰³ E. Fortin³⁷ A. W. Fortman^{18a}
M. G. Foti^{18a} L. Fountas^{9,r} D. Fournier⁶⁷ H. Fox⁹³ P. Francavilla^{75a,75b} S. Francescato⁶² S. Franchellucci⁵⁷
M. Franchini^{24b,24a} S. Franchino^{64a} D. Francis³⁷ L. Franco¹¹⁶ V. Franco Lima³⁷ L. Franconi⁴⁹ M. Franklin⁶²
G. Frattari²⁷ Y. Y. Frid¹⁵⁴ J. Friend⁶⁰ N. Fritzsche⁵¹ A. Froch⁵⁵ D. Froidevaux³⁷ J. A. Frost¹²⁹ Y. Fu^{63a}
S. Fuenzalida Garrido^{140f} M. Fujimoto¹⁰⁴ K. Y. Fung^{65a} E. Furtado De Simas Filho^{84e} M. Furukawa¹⁵⁶
J. Fuster¹⁶⁶ A. Gaa⁵⁶ A. Gabrielli^{24b,24a} A. Gabrielli¹⁵⁸ P. Gadow³⁷ G. Gagliardi^{58b,58a} L. G. Gagnon^{18a}
S. Gaid¹⁶³ S. Galantzan¹⁵⁴ E. J. Gallas¹²⁹ B. J. Gallop¹³⁷ K. K. Gan¹²² S. Ganguly¹⁵⁶ Y. Gao⁵³
F. M. Garay Walls^{140a,140b} B. Garcia³⁰ C. García¹⁶⁶ A. Garcia Alonso¹¹⁷ A. G. Garcia Caffaro¹⁷⁵
J. E. García Navarro¹⁶⁶ M. Garcia-Sciveres^{18a} G. L. Gardner¹³¹ R. W. Gardner⁴⁰ N. Garelli¹⁶¹ D. Garg⁸¹
R. B. Garg¹⁴⁶ J. M. Gargan⁵³ C. A. Garner¹⁵⁸ C. M. Garvey^{34a} V. K. Gassmann¹⁶¹ G. Gaudio^{74a} V. Gautam¹³
P. Gauzzi^{76a,76b} J. Gavranovic⁹⁵ I. L. Gavrilenko³⁸ A. Gavrilyuk³⁸ C. Gay¹⁶⁷ G. Gaycken¹²⁶ E. N. Gazis¹⁰
A. A. Geanta^{28b} C. M. Gee¹³⁹ A. Gekow¹²² C. Gemme^{58b} M. H. Genest⁶¹ A. D. Gentry¹¹⁵ S. George⁹⁷
W. F. George²¹ T. Geralis⁴⁷ P. Gessinger-Befurt³⁷ M. E. Geyik¹⁷⁴ M. Ghani¹⁷⁰ K. Ghorbanian⁹⁶
A. Ghosal¹⁴⁴ A. Ghosh¹⁶² A. Ghosh⁷ B. Giacobbe^{24b} S. Giagu^{76a,76b} T. Giani¹¹⁷ A. Giannini^{63a}
S. M. Gibson⁹⁷ M. Gignac¹³⁹ D. T. Gil^{87b} A. K. Gilbert^{87a} B. J. Gilbert⁴² D. Gillberg³⁵ G. Gilles¹¹⁷
L. Ginabat¹³⁰ D. M. Gingrich^{2,d} M. P. Giordani^{70a,70c} P. F. Giraud¹³⁸ G. Giugliarelli^{70a,70c} D. Giugni^{72a}
F. Giuli³⁷ I. Gkialas^{9,r} L. K. Gladilin³⁸ C. Glasman¹⁰¹ G. R. Gledhill¹²⁶ G. Glemža⁴⁹ M. Glisic¹²⁶
I. Gnesi^{44b,s} Y. Go³⁰ M. Goblirsch-Kolb³⁷ B. Gocke⁵⁰ D. Godin¹¹⁰ B. Gokturk^{22a} S. Goldfarb¹⁰⁷
T. Golling⁵⁷ M. G. D. Gololo^{34g} D. Golubkov³⁸ J. P. Gombas¹⁰⁹ A. Gomes^{133a,133b} G. Gomes Da Silva¹⁴⁴
A. J. Gomez Delegido¹⁶⁶ R. Gonçalves^{133a} L. Gonella²¹ A. Gongadze^{152c} F. Gonnella²¹ J. L. Gonski¹⁴⁶
R. Y. González Andana⁵³ S. González de la Hoz¹⁶⁶ R. Gonzalez Lopez⁹⁴ C. Gonzalez Renteria^{18a}
M. V. Gonzalez Rodrigues⁴⁹ R. Gonzalez Suarez¹⁶⁴ S. Gonzalez-Sevilla⁵⁷ L. Goossens³⁷ B. Gorini³⁷
E. Gorini^{71a,71b} A. Gorišek⁹⁵ T. C. Gosart¹³¹ A. T. Goshaw⁵² M. I. Gostkin³⁹ S. Goswami¹²⁴
C. A. Gottardo³⁷ S. A. Gotz¹¹¹ M. Gouighri^{36b} V. Goumarre⁴⁹ A. G. Goussiou¹⁴¹ N. Govender^{34c}
I. Grabowska-Bold^{87a} K. Graham³⁵ E. Gramstad¹²⁸ S. Grancagnolo^{71a,71b} C. M. Grant^{1,138} P. M. Gravila^{28f}
F. G. Gravili^{71a,71b} H. M. Gray^{18a} M. Greco^{71a,71b} M. J. Green¹ C. Grefe²⁵ A. S. Grefsrud¹⁷ I. M. Gregor⁴⁹
K. T. Greif¹⁶² P. Grenier¹⁴⁶ S. G. Grewe¹¹² A. A. Grillo¹³⁹ K. Grimm³² S. Grinstein^{13,t} J.-F. Grivaz⁶⁷
E. Gross¹⁷² J. Grosse-Knetter⁵⁶ J. C. Grundy¹²⁹ L. Guan¹⁰⁸ J. G. R. Guerrero Rojas¹⁶⁶ G. Guerrieri^{70a,70c}
R. Gugel¹⁰² J. A. M. Guhit¹⁰⁸ A. Guida¹⁹ E. Guilloton¹⁷⁰ S. Guindon³⁷ F. Guo^{14,114c} J. Guo^{63c} L. Guo⁴⁹
Y. Guo¹⁰⁸ R. Gupta¹³² S. Gurbuz²⁵ S. S. Gurdasani⁵⁵ G. Gustavino^{76a,76b} P. Gutierrez¹²³

L. F. Gutierrez Zagazeta¹³¹ M. Gutsche⁵¹ C. Gutschow⁹⁸ C. Gwenlan¹²⁹ C. B. Gwilliam⁹⁴ E. S. Haaland¹²⁸
 A. Haas¹²⁰ M. Habedank⁴⁹ C. Haber^{18a} H. K. Hadavand⁸ A. Hadeef⁵¹ S. Hadzic¹¹² A. I. Hagan⁹³
 J. J. Hahn¹⁴⁴ E. H. Haines⁹⁸ M. Haleem¹⁶⁹ J. Haley¹²⁴ J. J. Hall¹⁴² G. D. Hallowell¹⁰⁴ L. Halser²⁰
 K. Hamano¹⁶⁸ M. Hamer²⁵ G. N. Hamity⁵³ E. J. Hampshire⁹⁷ J. Han^{63b} K. Han^{63a} L. Han^{114a} L. Han^{63a}
 S. Han^{18a} Y. F. Han¹⁵⁸ K. Hanagaki⁸⁵ M. Hance¹³⁹ D. A. Hangal⁴² H. Hanif¹⁴⁵ M. D. Hank¹³¹
 J. B. Hansen⁴³ P. H. Hansen⁴³ K. Hara¹⁶⁰ D. Harada⁵⁷ T. Harenberg¹⁷⁴ S. Harkusha³⁸ M. L. Harris¹⁰⁵
 Y. T. Harris¹²⁹ J. Harrison¹³ N. M. Harrison¹²² P. F. Harrison¹⁷⁰ N. M. Hartman¹¹² N. M. Hartmann¹¹¹
 R. Z. Hasan^{97,137} Y. Hasegawa¹⁴³ S. Hassan¹⁷ R. Hauser¹⁰⁹ C. M. Hawkes²¹ R. J. Hawkings³⁷ Y. Hayashi¹⁵⁶
 S. Hayashida¹¹³ D. Hayden¹⁰⁹ C. Hayes¹⁰⁸ R. L. Hayes¹¹⁷ C. P. Hays¹²⁹ J. M. Hays⁹⁶ H. S. Hayward⁹⁴
 F. He^{63a} M. He^{14,114c} Y. He¹⁵⁷ Y. He⁴⁹ Y. He⁹⁸ N. B. Heatley⁹⁶ V. Hedberg¹⁰⁰ A. L. Heggelund¹²⁸
 N. D. Hehir^{96,a} C. Heidegger⁵⁵ K. K. Heidegger⁵⁵ J. Heilman³⁵ S. Heim⁴⁹ T. Heim^{18a} J. G. Heinlein¹³¹
 J. J. Heinrich¹²⁶ L. Heinrich^{112,u} J. Hejbal¹³⁴ A. Held¹⁷³ S. Hellesund¹⁷ C. M. Helling¹⁶⁷ S. Hellman^{48a,48b}
 R. C. W. Henderson⁹³ L. Henkelmann³³ A. M. Henriques Correia³⁷ H. Herde¹⁰⁰ Y. Hernández Jiménez¹⁴⁸
 L. M. Herrmann²⁵ T. Herrmann⁵¹ G. Herten⁵⁵ R. Hertenberger¹¹¹ L. Hervas³⁷ M. E. Hesping¹⁰²
 N. P. Hessey^{159a} M. Hidaoui^{36b} N. Hidic¹³⁶ E. Hill¹⁵⁸ S. J. Hillier²¹ J. R. Hinds¹⁰⁹ F. Hinterkeuser²⁵
 M. Hirose¹²⁷ S. Hirose¹⁶⁰ D. Hirschbuehl¹⁷⁴ T. G. Hitchings¹⁰³ B. Hiti⁹⁵ J. Hobbs¹⁴⁸ R. Hobincu^{28e}
 N. Hod¹⁷² M. C. Hodgkinson¹⁴² B. H. Hodgkinson¹²⁹ A. Hoecker³⁷ D. D. Hofer¹⁰⁸ J. Hofer⁴⁹ T. Holm²⁵
 M. Holzbock¹¹² L. B. A. H. Hommels³³ B. P. Honan¹⁰³ J. J. Hong⁶⁹ J. Hong^{63c} T. M. Hong¹³²
 B. H. Hooberman¹⁶⁵ W. H. Hopkins⁶ M. C. Hoppesch¹⁶⁵ Y. Horii¹¹³ S. Hou¹⁵¹ A. S. Howard⁹⁵ J. Howarth⁶⁰
 J. Hoya⁶ M. Hrabovsky¹²⁵ A. Hrynevich⁴⁹ T. Hryn'ova⁴ P. J. Hsu⁶⁶ S.-C. Hsu¹⁴¹ T. Hsu⁶⁷ M. Hu^{18a}
 Q. Hu^{63a} S. Huang^{65b} X. Huang^{14,114c} Y. Huang¹⁴² Y. Huang¹⁰² Y. Huang¹⁴ Z. Huang¹⁰³ Z. Hubacek¹³⁵
 M. Huebner²⁵ F. Huegging²⁵ T. B. Huffman¹²⁹ C. A. Hugli⁴⁹ M. Huhtinen³⁷ S. K. Huiberts¹⁷ R. Hulsken¹⁰⁶
 N. Huseynov¹² J. Huston¹⁰⁹ J. Huth⁶² R. Hyneman¹⁴⁶ G. Iacobucci⁵⁷ G. Iakovidis³⁰
 L. Iconomidou-Fayard⁶⁷ J. P. Iddon³⁷ P. Iengo^{73a,73b} R. Iguchi¹⁵⁶ Y. Iiyama¹⁵⁶ T. Iizawa¹²⁹ Y. Ikegami⁸⁵
 N. Ilic¹⁵⁸ H. Imam^{36a} M. Ince Lezki⁵⁷ T. Ingebretsen Carlson^{48a,48b} J. M. Inglis⁹⁶ G. Introzzi^{74a,74b}
 M. Iodice^{78a} V. Ippolito^{76a,76b} R. K. Irwin⁹⁴ M. Ishino¹⁵⁶ W. Islam¹⁷³ C. Issever^{19,49} S. Istin^{22a,v} H. Ito¹⁷¹
 R. Iuppa^{79a,79b} A. Ivina¹⁷² J. M. Izen⁴⁶ V. Izzo^{73a} P. Jacka¹³⁴ P. Jackson¹ C. S. Jagfeld¹¹¹ G. Jain^{159a}
 P. Jain⁴⁹ K. Jakobs⁵⁵ T. Jakoubek¹⁷² J. Jamieson⁶⁰ W. Jang¹⁵⁶ M. Javurkova¹⁰⁵ P. Jawahar¹⁰³ L. Jeanty¹²⁶
 J. Jejelava^{152a,w} P. Jenni^{55,x} C. E. Jessiman³⁵ C. Jia^{63b} J. Jia¹⁴⁸ X. Jia⁶² X. Jia^{14,114c} Z. Jia^{114a} C. Jiang⁵³
 S. Jiggins⁴⁹ J. Jimenez Pena¹³ S. Jin^{114a} A. Jinaru^{28b} O. Jinnouchi¹⁵⁷ P. Johansson¹⁴² K. A. Johns⁷
 J. W. Johnson¹³⁹ D. M. Jones¹⁴⁹ E. Jones⁴⁹ P. Jones³³ R. W. L. Jones⁹³ T. J. Jones⁹⁴ H. L. Joos^{56,37}
 R. Joshi¹²² J. Jovicevic¹⁶ X. Ju^{18a} J. J. Junggeburth¹⁰⁵ T. Junkermann^{64a} A. Juste Rozas¹³¹ M. K. Juzek⁸⁸
 S. Kabana^{140e} A. Kaczmarek⁸⁸ M. Kado¹¹² H. Kagan¹²² M. Kagan¹⁴⁶ A. Kahn¹³¹ C. Kahra¹⁰² T. Kaji¹⁵⁶
 E. Kajomovitz¹⁵³ N. Kakati¹⁷² I. Kalaitzidou⁵⁵ C. W. Kalderon³⁰ N. J. Kang¹³⁹ D. Kar^{34g} K. Karava¹²⁹
 M. J. Kareem^{159b} E. Karentzos⁵⁵ O. Karkout¹¹⁷ S. N. Karpov³⁹ Z. M. Karpova³⁹ V. Kartvelishvili⁹³
 A. N. Karyukhin³⁸ E. Kasimi¹⁵⁵ J. Katzy⁴⁹ S. Kaur³⁵ K. Kawade¹⁴³ M. P. Kawale¹²³ C. Kawamoto⁸⁹
 T. Kawamoto^{63a} E. F. Kay³⁷ F. I. Kaya¹⁶¹ S. Kazakos¹⁰⁹ V. F. Kazanin³⁸ Y. Ke¹⁴⁸ J. M. Keaveney^{34a}
 R. Keeler¹⁶⁸ G. V. Kehris⁶² J. S. Keller³⁵ A. S. Kelly⁹⁸ J. J. Kempster¹⁴⁹ P. D. Kennedy¹⁰² O. Kepka¹³⁴
 B. P. Kerridge¹³⁷ S. Kersten¹⁷⁴ B. P. Kerševan⁹⁵ L. Keszeghova^{29a} S. Ketabchi Haghghat¹⁵⁸ R. A. Khan¹³²
 A. Khanov¹²⁴ A. G. Kharlamov³⁸ T. Kharlamova³⁸ E. E. Khoda¹⁴¹ M. Kholodenko³⁸ T. J. Khoo¹⁹
 G. Khoriali¹⁶⁹ J. Khubua^{152b,a} Y. A. R. Khwaira¹³⁰ B. Kibirige^{34g} D. Kim⁶ D. W. Kim^{48a,48b} Y. K. Kim⁴⁰
 N. Kimura⁹⁸ M. K. Kingston⁵⁶ A. Kirchhoff⁵⁶ C. Kirfel²⁵ F. Kirfel²⁵ J. Kirk¹³⁷ A. E. Kiryunin¹¹²
 C. Kitsaki¹⁰ O. Kivernyk²⁵ M. Klassen¹⁶¹ C. Klein³⁵ L. Klein¹⁶⁹ M. H. Klein⁴⁵ S. B. Klein⁵⁷ U. Klein⁹⁴
 P. Klimek³⁷ A. Klimentov³⁰ T. Klioutchnikova³⁷ P. Kluit¹¹⁷ S. Kluth¹¹² E. Kneringer⁸⁰ T. M. Knight¹⁵⁸
 A. Knue⁵⁰ R. Kobayashi⁸⁹ D. Kobylanskii¹⁷² S. F. Koch¹²⁹ M. Kocian¹⁴⁶ P. Kodyš¹³⁶ D. M. Koeck¹²⁶
 P. T. Koenig²⁵ T. Koffas³⁵ O. Kolay⁵¹ I. Koletsou⁴ T. Komarek⁸⁸ K. Köneke⁵⁵ A. X. Y. Kong¹ T. Kono¹²¹
 N. Konstantinidis⁹⁸ P. Kontaxakis⁵⁷ B. Konya¹⁰⁰ R. Kopeliainsky⁴² S. Koperny^{87a} K. Korcyl⁸⁸
 K. Kordas^{155,y} A. Korn⁹⁸ S. Korn⁵⁶ I. Korolkov¹³ N. Korotkova³⁸ B. Kortman¹¹⁷ O. Kortner¹¹²
 S. Kortner¹¹² W. H. KostECKA¹¹⁸ V. V. Kostyukhin¹⁴⁴ A. Kotskechagia¹³⁸ A. Kotwal⁵² A. Koulouris³⁷

A. Kourkoumeli-Charalampidi^{74a,74b} C. Kourkoumelis⁹ E. Kourlitis^{112,u} O. Kovanda¹²⁶ R. Kowalewski¹⁶⁸
W. Kozanecki¹³⁸ A. S. Kozhin³⁸ V. A. Kramarenko³⁸ G. Kramberger⁹⁵ P. Kramer¹⁰² M. W. Krasny¹³⁰
A. Krasznahorkay³⁷ A. C. Kraus¹¹⁸ J. W. Kraus¹⁷⁴ J. A. Kremer⁴⁹ T. Kresse⁵¹ L. Kretschmann¹⁷⁴
J. Kretzschmar⁹⁴ K. Kreul¹⁹ P. Krieger¹⁵⁸ S. Krishnamurthy¹⁰⁵ M. Krivos¹³⁶ K. Krizka²¹ K. Kroeninger⁵⁰
H. Kroha¹¹² J. Kroll¹³⁴ J. Kroll¹³¹ K. S. Krowpman¹⁰⁹ U. Kruchonak³⁹ H. Krüger²⁵ N. Krumnack⁸²
M. C. Kruse⁵² O. Kuchinskaia³⁸ S. Kuday^{3a} S. Kuehn³⁷ R. Kuesters⁵⁵ T. Kuhl⁴⁹ V. Kukhtin³⁹
Y. Kulchitsky^{38,j} S. Kuleshov^{140d,140b} M. Kumar^{34g} N. Kumari⁴⁹ P. Kumari^{159b} A. Kupco¹³⁴ T. Kupfer⁵⁰
A. Kupich³⁸ O. Kuprash⁵⁵ H. Kurashige⁸⁶ L. L. Kurchaninov^{159a} O. Kurdyshev⁶⁷ Y. A. Kurochkin³⁸
A. Kurova³⁸ M. Kuze¹⁵⁷ A. K. Kvam¹⁰⁵ J. Kvita¹²⁵ T. Kwan¹⁰⁶ N. G. Kyriacou¹⁰⁸ L. A. O. Laatu¹⁰⁴
C. Lacasta¹⁶⁶ F. Lacava^{76a,76b} H. Lacker¹⁹ D. Lacour¹³⁰ N. N. Lad⁹⁸ E. Ladygin³⁹ A. Lafarge⁴¹
B. Laforge¹³⁰ T. Lagouri¹⁷⁵ F. Z. Lahbabi^{36a} S. Lai⁵⁶ J. E. Lambert¹⁶⁸ S. Lammers⁶⁹ W. Lampl⁷
C. Lampoudis^{155,y} G. Lamprinoudis¹⁰² A. N. Lancaster¹¹⁸ E. Lançon³⁰ U. Landgraf⁵⁵ M. P. J. Landon⁹⁶
V. S. Lang⁵⁵ O. K. B. Langrekken¹²⁸ A. J. Lankford¹⁶² F. Lanni³⁷ K. Lantzsch²⁵ A. Lanza^{74a} J. F. Laporte¹³⁸
T. Lari^{72a} F. Lasagni Manghi^{24b} M. Lassnig³⁷ V. Latonova¹³⁴ A. Laurier¹⁵³ S. D. Lawlor¹⁴² Z. Lawrence¹⁰³
R. Lazaridou¹⁷⁰ M. Lazzaroni^{72a,72b} B. Le¹⁰³ E. M. Le Boulicaut⁵² L. T. Le Pottier^{18a} B. Leban^{24b,24a}
A. Lebedev⁸² M. LeBlanc¹⁰³ F. Ledroit-Guillon⁶¹ S. C. Lee¹⁵¹ S. Lee^{48a,48b} T. F. Lee⁹⁴ L. L. Leeuw^{34c}
H. P. Lefebvre⁹⁷ M. Lefebvre¹⁶⁸ C. Leggett^{18a} G. Lehmann Miotto³⁷ M. Leigh⁵⁷ W. A. Leight¹⁰⁵
W. Leinonen¹¹⁶ A. Leisos^{155,z} M. A. L. Leite^{84c} C. E. Leitgeb¹⁹ R. Leitner¹³⁶ K. J. C. Leney⁴⁵ T. Lenz²⁵
S. Leone^{75a} C. Leonidopoulos⁵³ A. Leopold¹⁴⁷ R. Les¹⁰⁹ C. G. Lester³³ M. Levchenko³⁸ J. Levêque⁴
L. J. Levinson¹⁷² G. Levrini^{24b,24a} M. P. Lewicki⁸⁸ C. Lewis¹⁴¹ D. J. Lewis⁴ A. Li⁵ B. Li^{63b} C. Li^{63a}
C-Q. Li¹¹² H. Li^{63a} H. Li^{63b} H. Li^{114a} H. Li¹⁵ H. Li^{63b} J. Li^{63c} K. Li¹⁴¹ L. Li^{63c} M. Li^{14,114c}
S. Li^{14,114c} S. Li^{63d,63c} T. Li⁵ X. Li¹⁰⁶ Z. Li¹²⁹ Z. Li¹⁵⁶ Z. Li^{14,114c} S. Liang^{14,114c} Z. Liang¹⁴
M. Liberatore¹³⁸ B. Liberti^{77a} K. Lie^{65c} J. Lieber Marin^{84e} H. Lien⁶⁹ H. Lin¹⁰⁸ K. Lin¹⁰⁹ R. E. Lindley⁷
J. H. Lindon² J. Ling⁶² E. Lipeles¹³¹ A. Lipniacka¹⁷ A. Lister¹⁶⁷ J. D. Little⁶⁹ B. Liu¹⁴ B. X. Liu^{114b}
D. Liu^{63d,63c} E. H. L. Liu²¹ J. B. Liu^{63a} J. K. K. Liu³³ K. Liu^{63d} K. Liu^{63d,63c} M. Liu^{63a} M. Y. Liu^{63a}
P. Liu¹⁴ Q. Liu^{63d,141,63c} X. Liu^{63a} X. Liu^{63b} Y. Liu^{114b,114c} Y. L. Liu^{63b} Y. W. Liu^{63a} J. Llorente Merino¹⁴⁵
S. L. Lloyd⁹⁶ E. M. Lobodzinska⁴⁹ P. Loch⁷ T. Lohse¹⁹ K. Lohwasser¹⁴² E. Loiacono⁴⁹ M. Lokajicek^{134,a}
J. D. Lomas²¹ J. D. Long¹⁶⁵ I. Longarini¹⁶² R. Longo¹⁶⁵ I. Lopez Paz⁶⁸ A. Lopez Solis⁴⁹
N. Lorenzo Martinez⁴ A. M. Lory¹¹¹ M. Losada^{119a} G. Löschcke Centeno¹⁴⁹ O. Loseva³⁸ X. Lou^{48a,48b}
X. Lou^{14,114c} A. Lounis⁶⁷ P. A. Love⁹³ G. Lu^{14,114c} M. Lu⁶⁷ S. Lu¹³¹ Y. J. Lu⁶⁶ H. J. Lubatti¹⁴¹
C. Luci^{76a,76b} F. L. Lucio Alves^{114a} F. Luehring⁶⁹ I. Luise¹⁴⁸ O. Lukianchuk⁶⁷ O. Lundberg¹⁴⁷
B. Lund-Jensen^{147,a} N. A. Luongo⁶ M. S. Lutz³⁷ A. B. Lux²⁶ D. Lynn³⁰ R. Lysak¹³⁴ E. Lytken¹⁰⁰
V. Lyubushkin³⁹ T. Lyubushkina³⁹ M. M. Lyukova¹⁴⁸ M. Firdaus M. Soberi⁵³ H. Ma³⁰ K. Ma^{63a}
L. L. Ma^{63b} W. Ma^{63a} Y. Ma¹²⁴ J. C. MacDonald¹⁰² P. C. Machado De Abreu Farias^{84e} R. Madar⁴¹
T. Madula⁹⁸ J. Maeda⁸⁶ T. Maeno³⁰ H. Maguire¹⁴² V. Maiboroda¹³⁸ A. Maio^{133a,133b,133d} K. Maj^{87a}
O. Majersky⁴⁹ S. Majewski¹²⁶ N. Makovec⁶⁷ V. Maksimovic¹⁶ B. Malaescu¹³⁰ Pa. Malecki⁸⁸
V. P. Maleev³⁸ F. Malek^{61,aa} M. Mali⁹⁵ D. Malito⁹⁷ U. Mallik⁸¹ S. Maltezos¹⁰ S. Malyukov³⁹ J. Mamuzic¹³
G. Mancini⁵⁴ M. N. Mancini²⁷ G. Manco^{74a,74b} J. P. Mandalia⁹⁶ S. S. Mandary¹⁴⁹ I. Mandić⁹⁵
L. Manhaes de Andrade Filho^{84a} I. M. Maniatis¹⁷² J. Manjarres Ramos⁹¹ D. C. Mankad¹⁷² A. Mann¹¹¹
S. Manzoni³⁷ L. Mao^{63c} X. Mapekula^{34c} A. Marantis^{155,z} G. Marchiori⁵ M. Marcisovsky¹³⁴ C. Marcon^{72a}
M. Marinescu²¹ S. Marium⁴⁹ M. Marjanovic¹²³ A. Markhoos⁵⁵ M. Markovitch⁶⁷ E. J. Marshall⁹³
Z. Marshall^{18a} S. Marti-Garcia¹⁶⁶ J. Martin⁹⁸ T. A. Martin¹³⁷ V. J. Martin⁵³ B. Martin dit Latour¹⁷
L. Martinelli^{76a,76b} M. Martinez^{13,t} P. Martinez Agullo¹⁶⁶ V. I. Martinez Outschoorn¹⁰⁵ P. Martinez Suarez¹³
S. Martin-Haugh¹³⁷ G. Martinovicova¹³⁶ V. S. Martoiu^{28b} A. C. Martyniuk⁹⁸ A. Marzin³⁷ D. Mascione^{79a,79b}
L. Masetti¹⁰² T. Mashimo¹⁵⁶ J. Masik¹⁰³ A. L. Maslennikov³⁸ P. Massarotti^{73a,73b} P. Mastrandrea^{75a,75b}
A. Mastroberardino^{44b,44a} T. Masubuchi¹⁵⁶ T. Mathisen¹⁶⁴ J. Matousek¹³⁶ N. Matsuzawa¹⁵⁶ J. Maurer^{28b}
A. J. Maury⁶⁷ B. Maček⁹⁵ D. A. Maximov³⁸ A. E. May¹⁰³ R. Mazini¹⁵¹ I. Maznas¹¹⁸ M. Mazza¹⁰⁹
S. M. Mazza¹³⁹ E. Mazzeo^{72a,72b} C. Mc Ginn³⁰ J. P. Mc Gowan¹⁶⁸ S. P. Mc Kee¹⁰⁸ C. C. McCracken¹⁶⁷
E. F. McDonald¹⁰⁷ A. E. McDougall¹¹⁷ J. A. Mcfayden¹⁴⁹ R. P. McGovern¹³¹ R. P. Mckenzie^{34g}

T. C. McLachlan⁴⁹ D. J. Mclaughlin⁹⁸ S. J. McMahon¹³⁷ C. M. Mcpartland⁹⁴ R. A. McPherson^{168,n}
 S. Mehlhase¹¹¹ A. Mehta⁹⁴ D. Melini¹⁶⁶ B. R. Mellado Garcia^{34g} A. H. Melo⁵⁶ F. Meloni⁴⁹
 A. M. Mendes Jacques Da Costa¹⁰³ H. Y. Meng¹⁵⁸ L. Meng⁹³ S. Menke¹¹² M. Mentink³⁷ E. Meoni^{44b,44a}
 G. Mercado¹¹⁸ S. Merianos¹⁵⁵ C. Merlassino^{70a,70c} L. Merola^{73a,73b} C. Meroni^{72a,72b} J. Metcalfe⁶
 A. S. Mete⁶ E. Meuser¹⁰² C. Meyer⁶⁹ J-P. Meyer¹³⁸ R. P. Middleton¹³⁷ L. Mijović⁵³ G. Mikenberg¹⁷²
 M. Mikestikova¹³⁴ M. Mikuž⁹⁵ H. Mildner¹⁰² A. Milic³⁷ D. W. Miller⁴⁰ E. H. Miller¹⁴⁶ L. S. Miller³⁵
 A. Milov¹⁷² D. A. Milstead^{48a,48b} T. Min^{114a} A. A. Minaenko³⁸ I. A. Minashvili^{152b} L. Mince⁶⁰ A. I. Mincer¹²⁰
 B. Mindur^{87a} M. Mineev³⁹ Y. Mino⁸⁹ L. M. Mir¹³ M. Miralles Lopez⁶⁰ M. Mironova^{18a} A. Mishima¹⁵⁶
 M. C. Missio¹¹⁶ A. Mitra¹⁷⁰ V. A. Mitsou¹⁶⁶ Y. Mitsumori¹¹³ O. Miu¹⁵⁸ P. S. Miyagawa⁹⁶ T. Mkrtchyan^{64a}
 M. Mlinarevic⁹⁸ T. Mlinarevic⁹⁸ M. Mlynarikova³⁷ S. Mobius²⁰ P. Mogg¹¹¹ M. H. Mohamed Farook¹¹⁵
 A. F. Mohammed^{14,114c} S. Mohapatra⁴² G. Mokgatitwane^{34g} L. Moleri¹⁷² B. Mondal¹⁴⁴ S. Mondal¹³⁵
 K. Mönig⁴⁹ E. Monnier¹⁰⁴ L. Monsonis Romero¹⁶⁶ J. Montejo Berlingen¹³ M. Montella¹²² F. Montekali^{78a,78b}
 F. Monticelli⁹² S. Monzani^{70a,70c} N. Morange⁶⁷ A. L. Moreira De Carvalho⁴⁹ M. Moreno Llácer¹⁶⁶
 C. Moreno Martinez⁵⁷ P. Morettini^{58b} S. Morgenstern³⁷ M. Morii⁶² M. Morinaga¹⁵⁶ F. Morodei^{76a,76b}
 L. Morvaj³⁷ P. Moschovakos³⁷ B. Moser³⁷ M. Mosidze^{152b} T. Moskalets⁴⁵ P. Moskvitina¹¹⁶ J. Moss^{32,bb}
 P. Moszkowicz^{87a} A. Moussa^{36d} E. J. W. Moyse¹⁰⁵ O. Mtintsilana^{34g} S. Muanza¹⁰⁴ J. Mueller¹³²
 D. Muenstermann⁹³ R. Müller³⁷ G. A. Mullier¹⁶⁴ A. J. Mullin³³ J. J. Mullin¹³¹ D. P. Mungo¹⁵⁸
 D. Munoz Perez¹⁶⁶ F. J. Munoz Sanchez¹⁰³ M. Murin¹⁰³ W. J. Murray^{170,137} M. Muškinja⁹⁵ C. Mwewa³⁰
 A. G. Myagkov^{38,j} A. J. Myers⁸ G. Myers¹⁰⁸ M. Myska¹³⁵ B. P. Nachman^{18a} O. Nackenhorst⁵⁰ K. Nagai¹²⁹
 K. Nagano⁸⁵ J. L. Nagle^{30,o} E. Nagy¹⁰⁴ A. M. Nairz³⁷ Y. Nakahama⁸⁵ K. Nakamura⁸⁵ K. Nakkalil⁵
 H. Nanjo¹²⁷ E. A. Narayanan¹¹⁵ I. Naryshkin³⁸ L. Nasella^{72a,72b} M. Naseri³⁵ S. Nasri^{119b} C. Nass²⁵
 G. Navarro^{23a} J. Navarro-Gonzalez¹⁶⁶ R. Nayak¹⁵⁴ A. Nayaz¹⁹ P. Y. Nechaeva³⁸ S. Nechaeva^{24b,24a}
 F. Nechansky⁴⁹ L. Nedic¹²⁹ T. J. Neep²¹ A. Negri^{74a,74b} M. Negrini^{24b} C. Nellist¹¹⁷ C. Nelson¹⁰⁶
 K. Nelson¹⁰⁸ S. Nemecek¹³⁴ M. Nessi^{37,cc} M. S. Neubauer¹⁶⁵ F. Neuhaus¹⁰² J. Neundorff⁴⁹ P. R. Newman²¹
 C. W. Ng¹³² Y. W. Y. Ng⁴⁹ B. Ngair^{119a} H. D. N. Nguyen¹¹⁰ R. B. Nickerson¹²⁹ R. Nicolaidou¹³⁸
 J. Nielsen¹³⁹ M. Niemeier⁵⁶ J. Niemann⁵⁶ N. Nikiforou³⁷ V. Nikolaenko^{38,j} I. Nikolic-Audit¹³⁰
 K. Nikolopoulos²¹ P. Nilsson³⁰ I. Ninca⁴⁹ G. Ninio¹⁵⁴ A. Nisati^{76a} N. Nishu² R. Nisius¹¹² J-E. Nitschke⁵¹
 E. K. Nkadimeng^{34g} T. Nobe¹⁵⁶ T. Nommensen¹⁵⁰ M. B. Norfolk¹⁴² B. J. Norman³⁵ M. Noury^{36a}
 J. Novak⁹⁵ T. Novak⁹⁵ L. Novotny¹³⁵ R. Novotny¹¹⁵ L. Nozka¹²⁵ K. Ntekas¹⁶²
 N. M. J. Nunes De Moura Junior^{84b} J. Ocariz¹³⁰ A. Ochi⁸⁶ I. Ochoa^{133a} S. Oerdek^{49,dd} J. T. Offermann⁴⁰
 A. Ogrodnik¹³⁶ A. Oh¹⁰³ C. C. Ohm¹⁴⁷ H. Oide⁸⁵ R. Oishi¹⁵⁶ M. L. Ojeda⁴⁹ Y. Okumura¹⁵⁶
 L. F. Oleiro Seabra^{133a} I. Oleksiyuk⁵⁷ S. A. Olivares Pino^{140d} G. Oliveira Correa¹³ D. Oliveira Damazio³⁰
 D. Oliveira Goncalves^{84a} J. L. Oliver¹⁶² Ö. O. Öncel⁵⁵ A. P. O'Neill²⁰ A. Onofre^{133a,133e} P. U. E. Onyisi¹¹
 M. J. Oreglia⁴⁰ G. E. Orellana⁹² D. Orestano^{78a,78b} N. Orlando¹³ R. S. Orr¹⁵⁸ L. M. Osojnak¹³¹
 R. Ospanov^{63a} G. Otero y Garzon³¹ H. Otono⁹⁰ P. S. Ott^{64a} G. J. Ottino^{18a} M. Ouchrif^{36d} F. Ould-Saada¹²⁸
 T. Ovsianikova¹⁴¹ M. Owen⁶⁰ R. E. Owen¹³⁷ V. E. Ozcan^{22a} F. Ozturk⁸⁸ N. Ozturk⁸ S. Ozturk⁸³
 H. A. Pacey¹²⁹ A. Pacheco Pages¹³ C. Padilla Aranda¹³ G. Padovano^{76a,76b} S. Pagan Griso^{18a} G. Palacino⁶⁹
 A. Palazzo^{71a,71b} J. Pampel²⁵ J. Pan¹⁷⁵ T. Pan^{65a} D. K. Panchal¹¹ C. E. Pandini¹¹⁷ J. G. Panduro Vazquez¹³⁷
 H. D. Pandya¹ H. Pang¹⁵ P. Pani⁴⁹ G. Panizzo^{70a,70c} L. Panwar¹³⁰ L. Paolozzi⁵⁷ S. Parajuli¹⁶⁵
 A. Paramonov⁶ C. Paraskevopoulos⁵⁴ D. Paredes Hernandez^{65b} A. Pareti^{74a,74b} K. R. Park⁴² T. H. Park¹⁵⁸
 M. A. Parker³³ F. Parodi^{58b,58a} E. W. Parrish¹¹⁸ V. A. Parrish⁵³ J. A. Parsons⁴² U. Parzefall⁵⁵
 B. Pascual Dias¹¹⁰ L. Pascual Dominguez¹⁰¹ E. Pasqualucci^{76a} S. Passaggio^{58b} F. Pastore⁹⁷ P. Patel⁸⁸
 U. M. Patel⁵² J. R. Pater¹⁰³ T. Pauly³⁷ C. I. Pazos¹⁶¹ J. Pearkes¹⁴⁶ M. Pedersen¹²⁸ R. Pedro^{133a}
 S. V. Peleganchuk³⁸ O. Penc³⁷ E. A. Pender⁵³ G. D. Penn¹⁷⁵ K. E. Pensi¹¹¹ M. Penzin³⁸ B. S. Peralva^{84d}
 A. P. Pereira Peixoto¹⁴¹ L. Pereira Sanchez¹⁴⁶ D. V. Perepelitsa^{30,o} G. Perera¹⁰⁵ E. Perez Codina^{159a}
 M. Perganti¹⁰ H. Pernegger³⁷ S. Perrella^{76a,76b} O. Perrin⁴¹ K. Peters⁴⁹ R. F. Y. Peters¹⁰³ B. A. Petersen³⁷
 T. C. Petersen⁴³ E. Petit¹⁰⁴ V. Petousis¹³⁵ C. Petridou^{155,y} T. Petru¹³⁶ A. Petrukhin¹⁴⁴ M. Pettee^{18a}
 A. Petukhov³⁸ K. Petukhova³⁷ R. Pezoa^{140f} L. Pezzotti³⁷ G. Pezzullo¹⁷⁵ T. M. Pham¹⁷³ T. Pham¹⁰⁷
 P. W. Phillips¹³⁷ G. Piacquadio¹⁴⁸ E. Pianori^{18a} F. Piazza¹²⁶ R. Piegaia³¹ D. Pietreanu^{28b} A. D. Pilkington¹⁰³

M. Pinamonti ^{70a,70c} J. L. Pinfeld ² B. C. Pinheiro Pereira ^{133a} A. E. Pinto Pinoargote ¹³⁸ L. Pintucci ^{70a,70c}
K. M. Piper ¹⁴⁹ A. Pirttikoski ⁵⁷ D. A. Pizzi ³⁵ L. Pizzimento ^{65b} A. Pizzini ¹¹⁷ M.-A. Pleier ³⁰ V. Pleskot ¹³⁶
E. Plotnikova ³⁹ G. Poddar ⁹⁶ R. Poettgen ¹⁰⁰ L. Poggioli ¹³⁰ I. Pokharel ⁵⁶ S. Polacek ¹³⁶ G. Polesello ^{74a}
A. Poley ^{145,159a} A. Polini ^{24b} C. S. Pollard ¹⁷⁰ Z. B. Pollock ¹²² E. Pompa Pacchi ^{76a,76b} N. I. Pond ⁹⁸
D. Ponomarenko ¹¹⁶ L. Pontecorvo ³⁷ S. Popa ^{28a} G. A. Popeneciu ^{28d} A. Poreba ³⁷ D. M. Portillo Quintero ^{159a}
S. Pospisil ¹³⁵ M. A. Postill ¹⁴² P. Postolache ^{28c} K. Potamianos ¹⁷⁰ P. A. Potepa ^{87a} I. N. Potrap ³⁹ C. J. Potter ³³
H. Potti ¹⁵⁰ J. Poveda ¹⁶⁶ M. E. Pozo Astigarraga ³⁷ A. Prades Ibanez ¹⁶⁶ J. Pretel ⁵⁵ D. Price ¹⁰³
M. Primavera ^{71a} M. A. Principe Martin ¹⁰¹ R. Privara ¹²⁵ T. Procter ⁶⁰ M. L. Proffitt ¹⁴¹ N. Proklova ¹³¹
K. Prokofiev ^{65c} G. Proto ¹¹² J. Proudfoot ⁶ M. Przybycien ^{87a} W. W. Przygoda ^{87b} A. Psallidas ⁴⁷
J. E. Puddefoot ¹⁴² D. Pudzha ⁵⁵ D. Pyatiizbyantseva ³⁸ J. Qian ¹⁰⁸ D. Qichen ¹⁰³ Y. Qin ¹³ T. Qiu ⁵³
A. Quadt ⁵⁶ M. Queitsch-Maitland ¹⁰³ G. Quetant ⁵⁷ R. P. Quinn ¹⁶⁷ G. Rabanal Bolanos ⁶² D. Rafanoharana ⁵⁵
F. Raffaelli ^{77a,77b} F. Ragusa ^{72a,72b} J. L. Rainbolt ⁴⁰ J. A. Raine ⁵⁷ S. Rajagopalan ³⁰ E. Ramakoti ³⁸
I. A. Ramirez-Berend ³⁵ K. Ran ^{49,114c} N. P. Rapheeha ^{34g} H. Rasheed ^{28b} V. Raskina ¹³⁰ D. F. Rassloff ^{64a}
A. Rastogi ^{18a} S. Rave ¹⁰² S. Ravera ^{58b,58a} B. Ravina ⁵⁶ I. Ravinovich ¹⁷² M. Raymond ³⁷ A. L. Read ¹²⁸
N. P. Readioff ¹⁴² D. M. Rebuzzi ^{74a,74b} G. Redlinger ³⁰ A. S. Reed ¹¹² K. Reeves ²⁷ J. A. Reidelsturz ¹⁷⁴
D. Reikher ¹⁵⁴ A. Rej ⁵⁰ C. Rembser ³⁷ M. Renda ^{28b} F. Renner ⁴⁹ A. G. Rennie ¹⁶² A. L. Rescia ⁴⁹
S. Resconi ^{72a} M. Ressegotti ^{58b,58a} S. Rettie ³⁷ J. G. Reyes Rivera ¹⁰⁹ E. Reynolds ^{18a} O. L. Rezanova ³⁸
P. Reznicek ¹³⁶ H. Riani ^{36d} N. Ribaric ⁹³ E. Ricci ^{79a,79b} R. Richter ¹¹² S. Richter ^{48a,48b} E. Richter-Was ^{87b}
M. Ridel ¹³⁰ S. Ridouani ^{36d} P. Rieck ¹²⁰ P. Riedler ³⁷ E. M. Riefel ^{48a,48b} J. O. Rieger ¹¹⁷ M. Rijssenbeek ¹⁴⁸
M. Rimoldi ³⁷ L. Rinaldi ^{24b,24a} P. Rincke ^{56,164} T. T. Rinn ³⁰ M. P. Rinnagel ¹¹¹ G. Ripellino ¹⁶⁴ I. Riu ¹³
J. C. Rivera Vergara ¹⁶⁸ F. Rizatdinova ¹²⁴ E. Rizvi ⁹⁶ B. R. Roberts ^{18a} S. H. Robertson ^{106,n} D. Robinson ³³
C. M. Robles Gajardo ^{140f} M. Robles Manzano ¹⁰² A. Robson ⁶⁰ A. Rocchi ^{77a,77b} C. Roda ^{75a,75b}
S. Rodriguez Bosca ³⁷ Y. Rodriguez Garcia ^{23a} A. Rodriguez Rodriguez ⁵⁵ A. M. Rodríguez Vera ¹¹⁸ S. Roe ³⁷
J. T. Roemer ³⁷ A. R. Roepe-Gier ¹³⁹ O. Røhne ¹²⁸ R. A. Rojas ¹⁰⁵ C. P. A. Roland ¹³⁰ J. Roloff ³⁰
A. Romaniouk ³⁸ E. Romano ^{74a,74b} M. Romano ^{24b} A. C. Romero Hernandez ¹⁶⁵ N. Rompotis ⁹⁴ L. Roos ¹³⁰
S. Rosati ^{76a} B. J. Rosser ⁴⁰ E. Rossi ¹²⁹ E. Rossi ^{73a,73b} L. P. Rossi ⁶² L. Rossini ⁵⁵ R. Rosten ¹²² M. Rotaru ^{28b}
B. Rottler ⁵⁵ C. Rougier ⁹¹ D. Rousseau ⁶⁷ D. Rousso ⁴⁹ A. Roy ¹⁶⁵ S. Roy-Garand ¹⁵⁸ A. Rozanov ¹⁰⁴
Z. M. A. Rozario ⁶⁰ Y. Rozen ¹⁵³ A. Rubio Jimenez ¹⁶⁶ A. J. Ruby ⁹⁴ V. H. Ruelas Rivera ¹⁹ T. A. Ruggeri ¹
A. Ruggiero ¹²⁹ A. Ruiz-Martinez ¹⁶⁶ A. Rummler ³⁷ Z. Rurikova ⁵⁵ N. A. Rusakovich ³⁹ H. L. Russell ¹⁶⁸
G. Russo ^{76a,76b} J. P. Rutherford ⁷ S. Rutherford Colmenares ³³ M. Rybar ¹³⁶ E. B. Rye ¹²⁸ A. Ryzhov ⁴⁵
J. A. Sabater Iglesias ⁵⁷ P. Sabatini ¹⁶⁶ H. F-W. Sadrozinski ¹³⁹ F. Safai Tehrani ^{76a} B. Safarzadeh Samani ¹³⁷
S. Saha ¹ M. Sahinsoy ¹¹² A. Saibel ¹⁶⁶ M. Saimpert ¹³⁸ M. Saito ¹⁵⁶ T. Saito ¹⁵⁶ A. Sala ^{72a,72b} D. Salamani ³⁷
A. Salnikov ¹⁴⁶ J. Salt ¹⁶⁶ A. Salvador Salas ¹⁵⁴ D. Salvatore ^{44b,44a} F. Salvatore ¹⁴⁹ A. Salzburger ³⁷
D. Sammel ⁵⁵ E. Sampson ⁹³ D. Sampsonidis ^{155,y} D. Sampsonidou ¹²⁶ J. Sánchez ¹⁶⁶ V. Sanchez Sebastian ¹⁶⁶
H. Sandaker ¹²⁸ C. O. Sander ⁴⁹ J. A. Sandesara ¹⁰⁵ M. Sandhoff ¹⁷⁴ C. Sandoval ^{23b} L. Sanfilippo ^{64a}
D. P. C. Sankey ¹³⁷ T. Sano ⁸⁹ A. Sansoni ⁵⁴ L. Santi ^{37,76b} C. Santoni ⁴¹ H. Santos ^{133a,133b} A. Santra ¹⁷²
E. Sanzani ^{24b,24a} K. A. Saoucha ¹⁶³ J. G. Saraiva ^{133a,133d} J. Sardain ⁷ O. Sasaki ⁸⁵ K. Sato ¹⁶⁰ C. Sauer ^{64b}
E. Sauvan ⁴ P. Savard ^{158,d} R. Sawada ¹⁵⁶ C. Sawyer ¹³⁷ L. Sawyer ⁹⁹ C. Sbarra ^{24b} A. Sbrizzi ^{24b,24a}
T. Scanlon ⁹⁸ J. Schaarschmidt ¹⁴¹ U. Schäfer ¹⁰² A. C. Schaffer ^{67,45} D. Schaile ¹¹¹ R. D. Schamberger ¹⁴⁸
C. Scharf ¹⁹ M. M. Schefer ²⁰ V. A. Schegelsky ³⁸ D. Scheirich ¹³⁶ M. Schernau ¹⁶² C. Scheulen ⁵⁶
C. Schiavi ^{58b,58a} M. Schioppa ^{44b,44a} B. Schlag ^{146,ee} K. E. Schleicher ⁵⁵ S. Schlenker ³⁷ J. Schmeing ¹⁷⁴
M. A. Schmidt ¹⁷⁴ K. Schmieden ¹⁰² C. Schmitt ¹⁰² N. Schmitt ¹⁰² S. Schmitt ⁴⁹ L. Schoeffel ¹³⁸
A. Schoening ^{64b} P. G. Scholer ³⁵ E. Schopf ¹²⁹ M. Schott ²⁵ J. Schovancova ³⁷ S. Schramm ⁵⁷ T. Schroer ⁵⁷
H-C. Schultz-Coulon ^{64a} M. Schumacher ⁵⁵ B. A. Schumm ¹³⁹ Ph. Schune ¹³⁸ A. J. Schuy ¹⁴¹ H. R. Schwartz ¹³⁹
A. Schwartzman ¹⁴⁶ T. A. Schwarz ¹⁰⁸ Ph. Schwemling ¹³⁸ R. Schwienhorst ¹⁰⁹ F. G. Sciacca ²⁰ A. Sciandra ³⁰
G. Sciolla ²⁷ F. Scuri ^{75a} C. D. Sebastiani ⁹⁴ K. Sedlaczek ¹¹⁸ S. C. Seidel ¹¹⁵ A. Seiden ¹³⁹ B. D. Seidlitz ⁴²
C. Seitz ⁴⁹ J. M. Seixas ^{84b} G. Sekhniaidze ^{73a} L. Selem ⁶¹ N. Semprini-Cesari

- M. Shapiro^{18a}, A. Sharma³⁷, A. S. Sharma¹⁶⁷, P. Sharma⁸¹, P. B. Shatalov³⁸, K. Shaw¹⁴⁹, S. M. Shaw¹⁰³, Q. Shen^{63c}, D. J. Sheppard¹⁴⁵, P. Sherwood⁹⁸, L. Shi⁹⁸, X. Shi¹⁴, C. O. Shimmin¹⁷⁵, J. D. Shinner⁹⁷, I. P. J. Shipsey¹²⁹, S. Shirabe⁹⁰, M. Shiyakova^{39,ff}, M. J. Shochet⁴⁰, J. Shojaii¹⁰⁷, D. R. Shope¹²⁸, B. Shrestha¹²³, S. Shrestha^{122,gg}, M. J. Shroff¹⁶⁸, P. Sicho¹³⁴, A. M. Sickles¹⁶⁵, E. Sideras Haddad^{34g}, A. C. Sidley¹¹⁷, A. Sidoti^{24b}, F. Siegert⁵¹, Dj. Sijacki¹⁶, F. Sili⁹², J. M. Silva⁵³, I. Silva Ferreira^{84b}, M. V. Silva Oliveira³⁰, S. B. Silverstein^{48a}, S. Simion⁶⁷, R. Simoniello³⁷, E. L. Simpson¹⁰³, H. Simpson¹⁴⁹, L. R. Simpson¹⁰⁸, N. D. Simpson¹⁰⁰, S. Simsek⁸³, S. Sindhu⁵⁶, P. Sinervo¹⁵⁸, S. Singh¹⁵⁸, S. Sinha⁴⁹, S. Sinha¹⁰³, M. Sioli^{24b,24a}, I. Siral³⁷, E. Sitnikova⁴⁹, J. Sjölin^{48a,48b}, A. Skaf⁵⁶, E. Skorda²¹, P. Skubic¹²³, M. Slawinska⁸⁸, V. Smakhtin¹⁷², B. H. Smart¹³⁷, S. Yu. Smirnov³⁸, Y. Smirnov³⁸, L. N. Smirnova^{38,j}, O. Smirnova¹⁰⁰, A. C. Smith⁴², D. R. Smith¹⁶², E. A. Smith⁴⁰, H. A. Smith¹²⁹, J. L. Smith¹⁰³, R. Smith¹⁴⁶, M. Smizanska⁹³, K. Smolek¹³⁵, A. A. Snesarev³⁸, S. R. Snider¹⁵⁸, H. L. Snoek¹¹⁷, S. Snyder³⁰, R. Sobie^{168,n}, A. Soffer¹⁵⁴, C. A. Solans Sanchez³⁷, E. Yu. Soldatov³⁸, U. Soldevila¹⁶⁶, A. A. Solodkov³⁸, S. Solomon²⁷, A. Soloshenko³⁹, K. Solovieva⁵⁵, O. V. Solovyanov⁴¹, P. Sommer³⁷, A. Sonay¹³, W. Y. Song^{159b}, A. Sopczak¹³⁵, A. L. Soppio⁹⁸, F. Sopkova^{29b}, J. D. Sorenson¹¹⁵, I. R. Sotarriva Alvarez¹⁵⁷, V. Sothilingam^{64a}, O. J. Soto Sandoval^{140c,140b}, S. Sottocornola⁶⁹, R. Soualah¹⁶³, Z. Soumami^{36e}, D. South⁴⁹, N. Soybelman¹⁷², S. Spagnolo^{71a,71b}, M. Spalla¹¹², D. Sperlich⁵⁵, G. Spigo³⁷, S. Spinali⁹³, B. Spisso^{73a,73b}, D. P. Spiteri⁶⁰, M. Spousta¹³⁶, E. J. Staats³⁵, R. Stamen^{64a}, A. Stampekiš²¹, M. Standke²⁵, E. Stanecka⁸⁸, W. Stanek-Maslouska⁴⁹, M. V. Stange⁵¹, B. Stanislaus^{18a}, M. M. Stanitzki⁴⁹, B. Stapf⁴⁹, E. A. Starchenko³⁸, G. H. Stark¹³⁹, J. Stark⁹¹, P. Staroba¹³⁴, P. Starovoitov^{64a}, S. Stärz¹⁰⁶, R. Staszewski⁸⁸, G. Stavropoulos⁴⁷, P. Steinberg³⁰, B. Stelzer^{145,159a}, H. J. Stelzer¹³², O. Stelzer-Chilton^{159a}, H. Stenzel⁵⁹, T. J. Stevenson¹⁴⁹, G. A. Stewart³⁷, J. R. Stewart¹²⁴, M. C. Stockton³⁷, G. Stoicea^{28b}, M. Stolarski^{133a}, S. Stonjek¹¹², A. Straessner⁵¹, J. Strandberg¹⁴⁷, S. Strandberg^{48a,48b}, M. Stratmann¹⁷⁴, M. Strauss¹²³, T. Streblner¹⁰⁴, P. Strizenc^{29b}, R. Ströhmer¹⁶⁹, D. M. Strom¹²⁶, R. Stroynowski⁴⁵, A. Strubig^{48a,48b}, S. A. Stucci³⁰, B. Stugu¹⁷, J. Stupak¹²³, N. A. Styles⁴⁹, D. Su¹⁴⁶, S. Su^{63a}, W. Su^{63d}, X. Su^{63a}, D. Suchy^{29a}, K. Sugizaki¹⁵⁶, V. V. Sulim³⁸, M. J. Sullivan⁹⁴, D. M. S. Sultan¹²⁹, L. Sultanaliyeva³⁸, S. Sultansoy^{3b}, T. Sumida⁸⁹, S. Sun¹⁷³, O. Sunneborn Gudnadottir¹⁶⁴, N. Sur¹⁰⁴, M. R. Sutton¹⁴⁹, H. Suzuki¹⁶⁰, M. Svatos¹³⁴, M. Swiatlowski^{159a}, T. Swirski¹⁶⁹, I. Sykora^{29a}, M. Sykora¹³⁶, T. Sykora¹³⁶, D. Ta¹⁰², K. Tackmann^{49,dd}, A. Taffard¹⁶², R. Tafiout^{159a}, J. S. Tafoya Vargas⁶⁷, Y. Takubo⁸⁵, M. Talby¹⁰⁴, A. A. Talyshv³⁸, K. C. Tam^{65b}, N. M. Tamir¹⁵⁴, A. Tanaka¹⁵⁶, J. Tanaka¹⁵⁶, R. Tanaka⁶⁷, M. Tanasini¹⁴⁸, Z. Tao¹⁶⁷, S. Tapia Araya^{140f}, S. Tapprogge¹⁰², A. Tarek Abouelfadl Mohamed¹⁰⁹, S. Tarem¹⁵³, K. Tariq¹⁴, G. Tarna^{28b}, G. F. Tartarelli^{72a}, M. J. Tartarin⁹¹, P. Tas¹³⁶, M. Tasevsky¹³⁴, E. Tassi^{44b,44a}, A. C. Tate¹⁶⁵, G. Tateno¹⁵⁶, Y. Tayalati^{36e,hh}, G. N. Taylor¹⁰⁷, W. Taylor^{159b}, R. Teixeira De Lima¹⁴⁶, P. Teixeira-Dias⁹⁷, J. J. Teoh¹⁵⁸, K. Terashi¹⁵⁶, J. Terron¹⁰¹, S. Terzo¹³, M. Testa⁵⁴, R. J. Teuscher^{158,n}, A. Thaler⁸⁰, O. Theiner⁵⁷, N. Themistokleous⁵³, T. Thevenaux-Pelzer¹⁰⁴, O. Thielmann¹⁷⁴, D. W. Thomas⁹⁷, J. P. Thomas²¹, E. A. Thompson^{18a}, P. D. Thompson²¹, E. Thomson¹³¹, R. E. Thornberry⁴⁵, C. Tian^{63a}, Y. Tian⁵⁶, V. Tikhomirov^{38,j}, Yu. A. Tikhonov³⁸, S. Timoshenko³⁸, D. Timoshyn¹³⁶, E. X. L. Ting¹, P. Tipton¹⁷⁵, A. Tishelman-Charny³⁰, S. H. Tlou^{34g}, K. Todome¹⁵⁷, S. Todorova-Nova¹³⁶, S. Todt⁵¹, L. Toffolin^{70a,70c}, M. Togawa⁸⁵, J. Tojo⁹⁰, S. Tokár^{29a}, K. Tokushuku⁸⁵, O. Toldaiev⁶⁹, R. Tombs³³, M. Tomoto^{85,113}, L. Tompkins^{146,ee}, K. W. Topolnicki^{87b}, E. Torrence¹²⁶, H. Torres⁹¹, E. Torró Pastor¹⁶⁶, M. Toscani³¹, C. Toscirri⁴⁰, M. Tost¹¹, D. R. Tovey¹⁴², I. S. Trandafir^{28b}, T. Trefzger¹⁶⁹, A. Tricoli³⁰, I. M. Trigger^{159a}, S. Trincaz-Duvoid¹³⁰, D. A. Trischuk²⁷, B. Trocmé⁶¹, A. Tropina³⁹, L. Truong^{34c}, M. Trzebinski⁸⁸, A. Trzupek⁸⁸, F. Tsai¹⁴⁸, M. Tsai¹⁰⁸, A. Tsiamis^{155,y}, P. V. Tsiarehsha³⁸, S. Tsigaridas^{159a}, A. Tsirigotis^{155,z}, V. Tsiskaridze¹⁵⁸, E. G. Tskhadadze^{152a}, M. Tsopoulou¹⁵⁵, Y. Tsujikawa⁸⁹, I. I. Tsukerman³⁸, V. Tsulaia^{18a}, S. Tsuno⁸⁵, K. Tsurii¹²¹, D. Tsybychev¹⁴⁸, Y. Tu^{65b}, A. Tudorache^{28b}, V. Tudorache^{28b}, A. N. Tuna⁶², S. Turchikhin^{58b,58a}, I. Turk Cakir^{3a}, R. Turra^{72a}, T. Turtuvshin^{39,ii}, P. M. Tuts⁴², S. Tzamarias^{155,y}, E. Tzovara¹⁰², F. Ukegawa¹⁶⁰, P. A. Ulloa Poblete^{140c,140b}, E. N. Umaka³⁰, G. Unal³⁷, A. Undrus³⁰, G. Unel¹⁶², J. Urban^{29b}, P. Urrejola^{140a}, G. Usai⁸, R. Ushioda¹⁵⁷, M. Usman¹¹⁰, Z. Uysal⁸³, V. Vacek¹³⁵, B. Vachon¹⁰⁶, T. Vafeiadis³⁷, A. Vaitkus⁹⁸, C. Valderanis¹¹¹, E. Valdes Santurio^{48a,48b}, M. Valente^{159a}, S. Valentinetti^{24b,24a}, A. Valero¹⁶⁶, E. Valiente Moreno¹⁶⁶, A. Vallier⁹¹, J. A. Valls Ferrer¹⁶⁶, D. R. Van Arneman¹¹⁷, T. R. Van Daalen¹⁴¹, A. Van Der Graaf⁵⁰, P. Van Gemmeren⁶, M. Van Rijnbach³⁷, S. Van Stroud⁹⁸

I. Van Vulpen¹¹⁷ P. Vana¹³⁶ M. Vanadia^{77a,77b} W. Vandelli³⁷ E. R. Vandewall¹²⁴ D. Vannicola¹⁵⁴
 L. Vannoli⁵⁴ R. Vari^{76a} E. W. Varnes⁷ C. Varni^{18b} T. Varol¹⁵¹ D. Varouchas⁶⁷ L. Varriale¹⁶⁶
 K. E. Varvell¹⁵⁰ M. E. Vasile^{28b} L. Vaslin⁸⁵ G. A. Vasquez¹⁶⁸ A. Vasyukov³⁹ L. M. Vaughan¹²⁴ R. Vavricka¹⁰²
 T. Vazquez Schroeder³⁷ J. Veatch³² V. Vecchio¹⁰³ M. J. Veen¹⁰⁵ I. Veliscek³⁰ L. M. Veloce¹⁵⁸
 F. Veloso^{133a,133c} S. Veneziano^{76a} A. Ventura^{71a,71b} S. Ventura Gonzalez¹³⁸ A. Verbitskyi¹¹² M. Verducci^{75a,75b}
 C. Vergis⁹⁶ M. Verissimo De Araujo^{84b} W. Verkerke¹¹⁷ J. C. Vermeulen¹¹⁷ C. Vernieri¹⁴⁶ M. Vessella¹⁰⁵
 M. C. Vetterli^{145,d} A. Vgenopoulos¹⁰² N. Viaux Maira^{140f} T. Vickey¹⁴² O. E. Vickey Boeriu¹⁴²
 G. H. A. Viehhauser¹²⁹ L. Vigani^{64b} M. Villa^{24b,24a} M. Villaplana Perez¹⁶⁶ E. M. Villhauer⁵³ E. Vilucchi⁵⁴
 M. G. Vinciter³⁵ A. Visibile¹¹⁷ C. Vittori³⁷ I. Vivarelli^{24b,24a} E. Voevodina¹¹² F. Vogel¹¹¹ J. C. Voigt⁵¹
 P. Vokac¹³⁵ Yu. Volkotrub^{87b} J. Von Ahnen⁴⁹ E. Von Toerne²⁵ B. Vormwald³⁷ V. Vorobel¹³⁶ K. Vorobev³⁸
 M. Vos¹⁶⁶ K. Voss¹⁴⁴ M. Vozak¹¹⁷ L. Vozdecky¹²³ N. Vranjes¹⁶ M. Vranjes Milosavljevic¹⁶
 M. Vreeswijk¹¹⁷ N. K. Vu^{63d,63c} R. Vuillermet³⁷ O. Vujinovic¹⁰² I. Vukotic⁴⁰ S. Wada¹⁶⁰ C. Wagner¹⁰⁵
 J. M. Wagner^{18a} W. Wagner¹⁷⁴ S. Wahdan¹⁷⁴ H. Wahlberg⁹² M. Wakida¹¹³ J. Walder¹³⁷ R. Walker¹¹¹
 W. Walkowiak¹⁴⁴ A. Wall¹³¹ E. J. Wallin¹⁰⁰ T. Wamorkar⁶ A. Z. Wang¹³⁹ C. Wang¹⁰² C. Wang¹¹
 H. Wang^{18a} J. Wang^{65c} P. Wang⁹⁸ R. Wang⁶² R. Wang⁶ S. M. Wang¹⁵¹ S. Wang^{63b} S. Wang¹⁴
 T. Wang^{63a} W. T. Wang⁸¹ W. Wang¹⁴ X. Wang^{114a} X. Wang¹⁶⁵ X. Wang^{63c} Y. Wang^{63d} Y. Wang^{114a}
 Y. Wang^{63a} Z. Wang¹⁰⁸ Z. Wang^{63d,52,63c} Z. Wang¹⁰⁸ A. Warburton¹⁰⁶ R. J. Ward²¹ N. Warrack⁶⁰
 S. Waterhouse⁹⁷ A. T. Watson²¹ H. Watson⁶⁰ M. F. Watson²¹ E. Watton^{60,137} G. Watts¹⁴¹ B. M. Waugh⁹⁸
 J. M. Webb⁵⁵ C. Weber³⁰ H. A. Weber¹⁹ M. S. Weber²⁰ S. M. Weber^{64a} C. Wei^{63a} Y. Wei⁵⁵
 A. R. Weidberg¹²⁹ E. J. Weik¹²⁰ J. Weingarten⁵⁰ C. Weiser⁵⁵ C. J. Wells⁴⁹ T. Wenaus³⁰ B. Wendland⁵⁰
 T. Wengler³⁷ N. S. Wenke¹¹² N. Wermes²⁵ M. Wessels^{64a} A. M. Wharton⁹³ A. S. White⁶² A. White⁸
 M. J. White¹ D. Whiteson¹⁶² L. Wickremasinghe¹²⁷ W. Wiedenmann¹⁷³ M. Wielers¹³⁷ C. Wiglesworth⁴³
 D. J. Wilbern¹²³ H. G. Wilkens³⁷ J. J. H. Wilkinson³³ D. M. Williams⁴² H. H. Williams¹³¹ S. Williams³³
 S. Willocq¹⁰⁵ B. J. Wilson¹⁰³ P. J. Windischhofer⁴⁰ F. I. Winkel³¹ F. Winklmeier¹²⁶ B. T. Winter⁵⁵
 J. K. Winter¹⁰³ M. Wittgen¹⁴⁶ M. Wobisch⁹⁹ T. Wojtkowski⁶¹ Z. Wolffs¹¹⁷ J. Wollrath¹⁶² M. W. Wolter⁸⁸
 H. Wolters^{133a,133c} M. C. Wong¹³⁹ E. L. Woodward⁴² S. D. Worm⁴⁹ B. K. Wosiek⁸⁸ K. W. Woźniak⁸⁸
 S. Wozniowski⁵⁶ K. Wraight⁶⁰ C. Wu²¹ M. Wu^{114b} M. Wu¹¹⁶ S. L. Wu¹⁷³ X. Wu⁵⁷ Y. Wu^{63a} Z. Wu⁴
 J. Wuerzinger^{112,u} T. R. Wyatt¹⁰³ B. M. Wynne⁵³ S. Xella⁴³ L. Xia^{114a} M. Xia¹⁵ M. Xie^{63a} S. Xin^{14,114c}
 A. Xiong¹²⁶ J. Xiong^{18a} D. Xu¹⁴ H. Xu^{63a} L. Xu^{63a} R. Xu¹³¹ T. Xu¹⁰⁸ Y. Xu¹⁵ Z. Xu⁵³ Z. Xu^{114a}
 B. Yabsley¹⁵⁰ S. Yacoob^{34a} Y. Yamaguchi¹⁵⁷ E. Yamashita¹⁵⁶ H. Yamauchi¹⁶⁰ T. Yamazaki^{18a}
 Y. Yamazaki⁸⁶ J. Yan^{63c} S. Yan⁶⁰ Z. Yan¹⁰⁵ H. J. Yang^{63c,63d} H. T. Yang^{63a} S. Yang^{63a} T. Yang^{65c}
 X. Yang³⁷ X. Yang¹⁴ Y. Yang⁴⁵ Y. Yang^{63a} Z. Yang^{63a} W-M. Yao^{18a} H. Ye^{114a} H. Ye⁵⁶ J. Ye¹⁴ S. Ye³⁰
 X. Ye^{63a} Y. Yeh⁹⁸ I. Yeletsikh³⁹ B. Yeo^{18b} M. R. Yexley⁹⁸ T. P. Yildirim¹²⁹ P. Yin⁴² K. Yorita¹⁷¹
 S. Younas^{28b} C. J. S. Young³⁷ C. Young¹⁴⁶ C. Yu^{14,114c} Y. Yu^{63a} J. Yuan^{14,114c} M. Yuan¹⁰⁸ R. Yuan^{63d,63c}
 L. Yue⁹⁸ M. Zaazoua^{63a} B. Zabinski⁸⁸ E. Zaid⁵³ Z. K. Zak⁸⁸ T. Zakareishvili¹⁶⁶ S. Zambito⁵⁷
 J. A. Zamora Saa^{140d,140b} J. Zang¹⁵⁶ D. Zanzi⁵⁵ O. Zaplatilek¹³⁵ C. Zeitnitz¹⁷⁴ H. Zeng¹⁴ J. C. Zeng¹⁶⁵
 D. T. Zenger Jr.²⁷ O. Zenin³⁸ T. Ženiš^{29a} S. Zenz⁹⁶ S. Zerradi^{36a} D. Zerwas⁶⁷ M. Zhai^{14,114c} D. F. Zhang¹⁴²
 J. Zhang^{63b} J. Zhang⁶ K. Zhang^{14,114c} L. Zhang^{63a} L. Zhang^{114a} P. Zhang^{14,114c} R. Zhang¹⁷³ S. Zhang¹⁰⁸
 S. Zhang⁹¹ T. Zhang¹⁵⁶ X. Zhang^{63c} X. Zhang^{63b} Y. Zhang^{63c} Y. Zhang⁹⁸ Y. Zhang^{114a} Z. Zhang^{18a}
 Z. Zhang^{63b} Z. Zhang⁶⁷ H. Zhao¹⁴¹ T. Zhao^{63b} Y. Zhao¹³⁹ Z. Zhao^{63a} Z. Zhao^{63a} A. Zhemchugov³⁹
 J. Zheng^{114a} K. Zheng¹⁶⁵ X. Zheng^{63a} Z. Zheng¹⁴⁶ D. Zhong¹⁶⁵ B. Zhou¹⁰⁸ H. Zhou⁷ N. Zhou^{63c}
 Y. Zhou¹⁵ Y. Zhou^{114a} Y. Zhou⁷ C. G. Zhu^{63b} J. Zhu¹⁰⁸ X. Zhu^{63d} Y. Zhu^{63c} Y. Zhu^{63a} X. Zhuang¹⁴
 K. Zhukov³⁸ N. I. Zimine³⁹ J. Zinsser^{64b} M. Ziolkowski¹⁴⁴ L. Živković¹⁶ A. Zoccoli^{24b,24a} K. Zoch⁶²
 T. G. Zorbos¹⁴² O. Zormpa⁴⁷ W. Zou⁴² and L. Zwalinski³⁷

(ATLAS Collaboration)

¹Department of Physics, University of Adelaide, Adelaide, Australia²Department of Physics, University of Alberta, Edmonton, Alberta, Canada^{3a}Department of Physics, Ankara University, Ankara, Türkiye

- ^{3b}*Division of Physics, TOBB University of Economics and Technology, Ankara, Türkiye*
⁴*LAPP, Université Savoie Mont Blanc, CNRS/IN2P3, Annecy, France*
⁵*APC, Université Paris Cité, CNRS/IN2P3, Paris, France*
- ⁶*High Energy Physics Division, Argonne National Laboratory, Argonne, Illinois, USA*
⁷*Department of Physics, University of Arizona, Tucson, Arizona, USA*
⁸*Department of Physics, University of Texas at Arlington, Arlington, Texas, USA*
⁹*Physics Department, National and Kapodistrian University of Athens, Athens, Greece*
¹⁰*Physics Department, National Technical University of Athens, Zografou, Greece*
¹¹*Department of Physics, University of Texas at Austin, Austin, Texas, USA*
¹²*Institute of Physics, Azerbaijan Academy of Sciences, Baku, Azerbaijan*
- ¹³*Institut de Física d'Altes Energies (IFAE), Barcelona Institute of Science and Technology, Barcelona, Spain*
¹⁴*Institute of High Energy Physics, Chinese Academy of Sciences, Beijing, China*
¹⁵*Physics Department, Tsinghua University, Beijing, China*
¹⁶*Institute of Physics, University of Belgrade, Belgrade, Serbia*
¹⁷*Department for Physics and Technology, University of Bergen, Bergen, Norway*
- ^{18a}*Physics Division, Lawrence Berkeley National Laboratory, Berkeley, California, USA*
^{18b}*University of California, Berkeley, California, USA*
¹⁹*Institut für Physik, Humboldt Universität zu Berlin, Berlin, Germany*
- ²⁰*Albert Einstein Center for Fundamental Physics and Laboratory for High Energy Physics, University of Bern, Bern, Switzerland*
- ²¹*School of Physics and Astronomy, University of Birmingham, Birmingham, United Kingdom*
^{22a}*Department of Physics, Bogazici University, Istanbul, Türkiye*
^{22b}*Department of Physics Engineering, Gaziantep University, Gaziantep, Türkiye*
^{22c}*Department of Physics, Istanbul University, Istanbul, Türkiye*
- ^{23a}*Facultad de Ciencias y Centro de Investigaciones, Universidad Antonio Nariño, Bogotá, Colombia*
^{23b}*Departamento de Física, Universidad Nacional de Colombia, Bogotá, Colombia*
^{24a}*Dipartimento di Fisica e Astronomia A. Righi, Università di Bologna, Bologna, Italy*
^{24b}*INFN Sezione di Bologna, Bologna, Italy*
²⁵*Physikalisches Institut, Universität Bonn, Bonn, Germany*
²⁶*Department of Physics, Boston University, Boston, Massachusetts, USA*
²⁷*Department of Physics, Brandeis University, Waltham, Massachusetts, USA*
^{28a}*Transilvania University of Brasov, Brasov, Romania*
- ^{28b}*Horia Hulubei National Institute of Physics and Nuclear Engineering, Bucharest, Romania*
^{28c}*Department of Physics, Alexandru Ioan Cuza University of Iasi, Iasi, Romania*
^{28d}*National Institute for Research and Development of Isotopic and Molecular Technologies, Physics Department, Cluj-Napoca, Romania*
^{28e}*National University of Science and Technology Politehnica, Bucharest, Romania*
^{28f}*West University in Timisoara, Timisoara, Romania*
^{28g}*Faculty of Physics, University of Bucharest, Bucharest, Romania*
- ^{29a}*Faculty of Mathematics, Physics and Informatics, Comenius University, Bratislava, Slovak Republic*
^{29b}*Department of Subnuclear Physics, Institute of Experimental Physics of the Slovak Academy of Sciences, Kosice, Slovak Republic*
³⁰*Physics Department, Brookhaven National Laboratory, Upton, New York, USA*
- ³¹*Universidad de Buenos Aires, Facultad de Ciencias Exactas y Naturales, Departamento de Física, y CONICET, Instituto de Física de Buenos Aires (IFIBA), Buenos Aires, Argentina*
³²*California State University, California, USA*
³³*Cavendish Laboratory, University of Cambridge, Cambridge, United Kingdom*
^{34a}*Department of Physics, University of Cape Town, Cape Town, South Africa*
^{34b}*iThemba Labs, Western Cape, South Africa*
^{34c}*Department of Mechanical Engineering Science, University of Johannesburg, Johannesburg, South Africa*
- ^{34d}*National Institute of Physics, University of the Philippines Diliman, Diliman, Philippines*
^{34e}*University of South Africa, Department of Physics, Pretoria, South Africa*
^{34f}*University of Zululand, KwaDlangezwa, South Africa*
^{34g}*School of Physics, University of the Witwatersrand, Johannesburg, South Africa*
³⁵*Department of Physics, Carleton University, Ottawa, Ontario, Canada*
- ^{36a}*Faculté des Sciences Ain Chock, Université Hassan II de Casablanca, Casablanca, Morocco*
^{36b}*Faculté des Sciences, Université Ibn-Tofail, Kénitra, Morocco*
^{36c}*Faculté des Sciences Semlalia, Université Cadi Ayyad, LPHEA-Marrakech, Morocco*

- ^{36d}*LPMR, Faculté des Sciences, Université Mohamed Premier, Oujda, Morocco*
- ^{36c}*Faculté des sciences, Université Mohammed V, Rabat, Morocco*
- ^{36f}*Institute of Applied Physics, Mohammed VI Polytechnic University, Ben Guerir, Morocco*
- ³⁷*CERN, Geneva, Switzerland*
- ³⁸*Affiliated with an institute covered by a cooperation agreement with CERN*
- ³⁹*Affiliated with an international laboratory covered by a cooperation agreement with CERN*
- ⁴⁰*Enrico Fermi Institute, University of Chicago, Chicago, Illinois, USA*
- ⁴¹*LPC, Université Clermont Auvergne, CNRS/IN2P3, Clermont-Ferrand, France*
- ⁴²*Nevis Laboratory, Columbia University, Irvington, New York, USA*
- ⁴³*Niels Bohr Institute, University of Copenhagen, Copenhagen, Denmark*
- ^{44a}*Dipartimento di Fisica, Università della Calabria, Rende, Italy*
- ^{44b}*INFN Gruppo Collegato di Cosenza, Laboratori Nazionali di Frascati, Italy*
- ⁴⁵*Physics Department, Southern Methodist University, Dallas, Texas, USA*
- ⁴⁶*Physics Department, University of Texas at Dallas, Richardson, Texas, USA*
- ⁴⁷*National Centre for Scientific Research “Demokritos,” Agia Paraskevi, Greece*
- ^{48a}*Department of Physics, Stockholm University, Sweden*
- ^{48b}*Oskar Klein Centre, Stockholm, Sweden*
- ⁴⁹*Deutsches Elektronen-Synchrotron DESY, Hamburg and Zeuthen, Germany*
- ⁵⁰*Fakultät Physik, Technische Universität Dortmund, Dortmund, Germany*
- ⁵¹*Institut für Kern- und Teilchenphysik, Technische Universität Dresden, Dresden, Germany*
- ⁵²*Department of Physics, Duke University, Durham, North Carolina, USA*
- ⁵³*SUPA—School of Physics and Astronomy, University of Edinburgh, Edinburgh, United Kingdom*
- ⁵⁴*INFN e Laboratori Nazionali di Frascati, Frascati, Italy*
- ⁵⁵*Physikalisches Institut, Albert-Ludwigs-Universität Freiburg, Freiburg, Germany*
- ⁵⁶*II. Physikalisches Institut, Georg-August-Universität Göttingen, Göttingen, Germany*
- ⁵⁷*Département de Physique Nucléaire et Corpusculaire, Université de Genève, Genève, Switzerland*
- ^{58a}*Dipartimento di Fisica, Università di Genova, Genova, Italy*
- ^{58b}*INFN Sezione di Genova, Genova, Italy*
- ⁵⁹*II. Physikalisches Institut, Justus-Liebig-Universität Giessen, Giessen, Germany*
- ⁶⁰*SUPA—School of Physics and Astronomy, University of Glasgow, Glasgow, United Kingdom*
- ⁶¹*LPSC, Université Grenoble Alpes, CNRS/IN2P3, Grenoble INP, Grenoble, France*
- ⁶²*Laboratory for Particle Physics and Cosmology, Harvard University, Cambridge, Massachusetts, USA*
- ^{63a}*Department of Modern Physics and State Key Laboratory of Particle Detection and Electronics, University of Science and Technology of China, Hefei, China*
- ^{63b}*Institute of Frontier and Interdisciplinary Science and Key Laboratory of Particle Physics and Particle Irradiation (MOE), Shandong University, Qingdao, China*
- ^{63c}*School of Physics and Astronomy, Shanghai Jiao Tong University, Key Laboratory for Particle Astrophysics and Cosmology (MOE), SKLPPC, Shanghai, China*
- ^{63d}*Tsung-Dao Lee Institute, Shanghai, China*
- ^{63e}*School of Physics and Microelectronics, Zhengzhou University, China*
- ^{64a}*Kirchhoff-Institut für Physik, Ruprecht-Karls-Universität Heidelberg, Heidelberg, Germany*
- ^{64b}*Physikalisches Institut, Ruprecht-Karls-Universität Heidelberg, Heidelberg, Germany*
- ^{65a}*Department of Physics, Chinese University of Hong Kong, Shatin, N.T., Hong Kong, China*
- ^{65b}*Department of Physics, University of Hong Kong, Hong Kong, China*
- ^{65c}*Department of Physics and Institute for Advanced Study, Hong Kong University of Science and Technology, Clear Water Bay, Kowloon, Hong Kong, China*
- ⁶⁶*Department of Physics, National Tsing Hua University, Hsinchu, Taiwan*
- ⁶⁷*IJCLab, Université Paris-Saclay, CNRS/IN2P3, 91405, Orsay, France*
- ⁶⁸*Centro Nacional de Microelectrónica (IMB-CNM-CSIC), Barcelona, Spain*
- ⁶⁹*Department of Physics, Indiana University, Bloomington, Indiana, USA*
- ^{70a}*INFN Gruppo Collegato di Udine, Sezione di Trieste, Udine, Italy*
- ^{70b}*ICTP, Trieste, Italy*
- ^{70c}*Dipartimento Politecnico di Ingegneria e Architettura, Università di Udine, Udine, Italy*
- ^{71a}*INFN Sezione di Lecce, Lecce, Italy*
- ^{71b}*Dipartimento di Matematica e Fisica, Università del Salento, Lecce, Italy*
- ^{72a}*INFN Sezione di Milano, Milano, Italy*
- ^{72b}*Dipartimento di Fisica, Università di Milano, Milano, Italy*
- ^{73a}*INFN Sezione di Napoli, Napoli, Italy*
- ^{73b}*Dipartimento di Fisica, Università di Napoli, Napoli, Italy*
- ^{74a}*INFN Sezione di Pavia, Pavia, Italy*

- ^{74b}Dipartimento di Fisica, Università di Pavia, Pavia, Italy
^{75a}INFN Sezione di Pisa, Pisa, Italy
^{75b}Dipartimento di Fisica E. Fermi, Università di Pisa, Pisa, Italy
^{76a}INFN Sezione di Roma, Italy
^{76b}Dipartimento di Fisica, Sapienza Università di Roma, Roma, Italy
^{77a}INFN Sezione di Roma Tor Vergata, Roma, Italy
^{77b}Dipartimento di Fisica, Università di Roma Tor Vergata, Roma, Italy
^{78a}INFN Sezione di Roma Tre, Roma, Italy
^{78b}Dipartimento di Matematica e Fisica, Università Roma Tre, Roma, Italy
^{79a}INFN-TIFPA, Trento, Italy
^{79b}Università degli Studi di Trento, Trento, Italy
⁸⁰Universität Innsbruck, Department of Astro and Particle Physics, Innsbruck, Austria
⁸¹University of Iowa, Iowa City, Iowa, USA
⁸²Department of Physics and Astronomy, Iowa State University, Ames, Iowa, USA
⁸³Istinye University, Sariyer, Istanbul, Türkiye
^{84a}Departamento de Engenharia Elétrica, Universidade Federal de Juiz de Fora (UFJF), Juiz de Fora, Brazil
^{84b}Universidade Federal do Rio De Janeiro COPPE/EE/IF, Rio de Janeiro, Brazil
^{84c}Instituto de Física, Universidade de São Paulo, São Paulo, Brazil
^{84d}Rio de Janeiro State University, Rio de Janeiro, Brazil
^{84e}Federal University of Bahia, Bahia, Brazil
⁸⁵KEK, High Energy Accelerator Research Organization, Tsukuba, Japan
⁸⁶Graduate School of Science, Kobe University, Kobe, Japan
^{87a}AGH University of Krakow, Faculty of Physics and Applied Computer Science, Krakow, Poland
^{87b}Marian Smoluchowski Institute of Physics, Jagiellonian University, Krakow, Poland
⁸⁸Institute of Nuclear Physics Polish Academy of Sciences, Krakow, Poland
⁸⁹Faculty of Science, Kyoto University, Kyoto, Japan
⁹⁰Research Center for Advanced Particle Physics and Department of Physics, Kyushu University, Fukuoka, Japan
⁹¹L2IT, Université de Toulouse, CNRS/IN2P3, UPS, Toulouse, France
⁹²Instituto de Física La Plata, Universidad Nacional de La Plata and CONICET, La Plata, Argentina
⁹³Physics Department, Lancaster University, Lancaster, United Kingdom
⁹⁴Oliver Lodge Laboratory, University of Liverpool, Liverpool, United Kingdom
⁹⁵Department of Experimental Particle Physics, Jožef Stefan Institute and Department of Physics, University of Ljubljana, Ljubljana, Slovenia
⁹⁶School of Physics and Astronomy, Queen Mary University of London, London, United Kingdom
⁹⁷Department of Physics, Royal Holloway University of London, Egham, United Kingdom
⁹⁸Department of Physics and Astronomy, University College London, London, United Kingdom
⁹⁹Louisiana Tech University, Ruston, Louisiana, USA
¹⁰⁰Fysiska institutionen, Lunds universitet, Lund, Sweden
¹⁰¹Departamento de Física Teórica C-15 and CIAFF, Universidad Autónoma de Madrid, Madrid, Spain
¹⁰²Institut für Physik, Universität Mainz, Mainz, Germany
¹⁰³School of Physics and Astronomy, University of Manchester, Manchester, United Kingdom
¹⁰⁴CPPM, Aix-Marseille Université, CNRS/IN2P3, Marseille, France
¹⁰⁵Department of Physics, University of Massachusetts, Amherst, Massachusetts, USA
¹⁰⁶Department of Physics, McGill University, Montreal, Quebec, Canada
¹⁰⁷School of Physics, University of Melbourne, Victoria, Australia
¹⁰⁸Department of Physics, University of Michigan, Ann Arbor, Michigan, USA
¹⁰⁹Department of Physics and Astronomy, Michigan State University, East Lansing, Michigan, USA
¹¹⁰Group of Particle Physics, University of Montreal, Montreal, Quebec, Canada
¹¹¹Fakultät für Physik, Ludwig-Maximilians-Universität München, München, Germany
¹¹²Max-Planck-Institut für Physik (Werner-Heisenberg-Institut), München, Germany
¹¹³Graduate School of Science and Kobayashi-Maskawa Institute, Nagoya University, Nagoya, Japan
^{114a}Department of Physics, Nanjing University, Nanjing, China
^{114b}School of Science, Shenzhen Campus of Sun Yat-sen University, China
^{114c}University of Chinese Academy of Science (UCAS), Beijing, China
¹¹⁵Department of Physics and Astronomy, University of New Mexico, Albuquerque, New Mexico, USA
¹¹⁶Institute for Mathematics, Astrophysics and Particle Physics, Radboud University/Nikhef, Nijmegen, Netherlands
¹¹⁷Nikhef National Institute for Subatomic Physics and University of Amsterdam, Amsterdam, Netherlands

- ¹¹⁸*Department of Physics, Northern Illinois University, DeKalb, Illinois, USA*
^{119a}*New York University Abu Dhabi, Abu Dhabi, United Arab Emirates*
^{119b}*United Arab Emirates University, Al Ain, United Arab Emirates*
¹²⁰*Department of Physics, New York University, New York, New York, USA*
¹²¹*Ochanomizu University, Otsuka, Bunkyo-ku, Tokyo, Japan*
¹²²*The Ohio State University, Columbus, Ohio, USA*
¹²³*Homer L. Dodge Department of Physics and Astronomy, University of Oklahoma, Norman, Oklahoma, USA*
¹²⁴*Department of Physics, Oklahoma State University, Stillwater, Oklahoma, USA*
¹²⁵*Palacký University, Joint Laboratory of Optics, Olomouc, Czech Republic*
¹²⁶*Institute for Fundamental Science, University of Oregon, Eugene, Oregon, USA*
¹²⁷*Graduate School of Science, Osaka University, Osaka, Japan*
¹²⁸*Department of Physics, University of Oslo, Oslo, Norway*
¹²⁹*Department of Physics, Oxford University, Oxford, United Kingdom*
¹³⁰*LPNHE, Sorbonne Université, Université Paris Cité, CNRS/IN2P3, Paris, France*
¹³¹*Department of Physics, University of Pennsylvania, Philadelphia, Pennsylvania, USA*
¹³²*Department of Physics and Astronomy, University of Pittsburgh, Pittsburgh, Pennsylvania, USA*
^{133a}*Laboratório de Instrumentação e Física Experimental de Partículas—LIP, Lisboa, Portugal*
^{133b}*Departamento de Física, Faculdade de Ciências, Universidade de Lisboa, Lisboa, Portugal*
^{133c}*Departamento de Física, Universidade de Coimbra, Coimbra, Portugal*
^{133d}*Centro de Física Nuclear da Universidade de Lisboa, Lisboa, Portugal*
^{133e}*Departamento de Física, Universidade do Minho, Braga, Portugal*
^{133f}*Departamento de Física Teórica y del Cosmos, Universidad de Granada, Granada, Spain*
^{133g}*Departamento de Física, Instituto Superior Técnico, Universidade de Lisboa, Lisboa, Portugal*
¹³⁴*Institute of Physics of the Czech Academy of Sciences, Prague, Czech Republic*
¹³⁵*Czech Technical University in Prague, Prague, Czech Republic*
¹³⁶*Charles University, Faculty of Mathematics and Physics, Prague, Czech Republic*
¹³⁷*Particle Physics Department, Rutherford Appleton Laboratory, Didcot, United Kingdom*
¹³⁸*IRFU, CEA, Université Paris-Saclay, Gif-sur-Yvette, France*
¹³⁹*Santa Cruz Institute for Particle Physics, University of California Santa Cruz, Santa Cruz, California, USA*
^{140a}*Departamento de Física, Pontificia Universidad Católica de Chile, Santiago, Chile*
^{140b}*Millennium Institute for Subatomic physics at high energy frontier (SAPHIR), Santiago, Chile*
^{140c}*Instituto de Investigación Multidisciplinario en Ciencia y Tecnología, y Departamento de Física, Universidad de La Serena, Chile*
^{140d}*Universidad Andres Bello, Department of Physics, Santiago, Chile*
^{140e}*Instituto de Alta Investigación, Universidad de Tarapacá, Arica, Chile*
^{140f}*Departamento de Física, Universidad Técnica Federico Santa María, Valparaíso, Chile*
¹⁴¹*Department of Physics, University of Washington, Seattle, Washington, USA*
¹⁴²*Department of Physics and Astronomy, University of Sheffield, Sheffield, United Kingdom*
¹⁴³*Department of Physics, Shinshu University, Nagano, Japan*
¹⁴⁴*Department Physik, Universität Siegen, Siegen, Germany*
¹⁴⁵*Department of Physics, Simon Fraser University, Burnaby, British Columbia, Canada*
¹⁴⁶*SLAC National Accelerator Laboratory, Stanford, California, USA*
¹⁴⁷*Department of Physics, Royal Institute of Technology, Stockholm, Sweden*
¹⁴⁸*Departments of Physics and Astronomy, Stony Brook University, Stony Brook, New York, USA*
¹⁴⁹*Department of Physics and Astronomy, University of Sussex, Brighton, United Kingdom*
¹⁵⁰*School of Physics, University of Sydney, Sydney, Australia*
¹⁵¹*Institute of Physics, Academia Sinica, Taipei, Taiwan*
^{152a}*E. Andronikashvili Institute of Physics, Iv. Javakhishvili Tbilisi State University, Tbilisi, Georgia*
^{152b}*High Energy Physics Institute, Tbilisi State University, Tbilisi, Georgia*
^{152c}*University of Georgia, Tbilisi, Georgia*
¹⁵³*Department of Physics, Technion, Israel Institute of Technology, Haifa, Israel*
¹⁵⁴*Raymond and Beverly Sackler School of Physics and Astronomy, Tel Aviv University, Tel Aviv, Israel*
¹⁵⁵*Department of Physics, Aristotle University of Thessaloniki, Thessaloniki, Greece*
¹⁵⁶*International Center for Elementary Particle Physics and Department of Physics, University of Tokyo, Tokyo, Japan*
¹⁵⁷*Department of Physics, Tokyo Institute of Technology, Tokyo, Japan*
¹⁵⁸*Department of Physics, University of Toronto, Toronto, Ontario, Canada*
^{159a}*TRIUMF, Vancouver, British Columbia, Canada*

- ^{159b}*Department of Physics and Astronomy, York University, Toronto, Ontario, Canada*
¹⁶⁰*Division of Physics and Tomonaga Center for the History of the Universe, Faculty of Pure and Applied Sciences, University of Tsukuba, Tsukuba, Japan*
¹⁶¹*Department of Physics and Astronomy, Tufts University, Medford, Massachusetts, USA*
¹⁶²*Department of Physics and Astronomy, University of California Irvine, Irvine, California, USA*
¹⁶³*University of Sharjah, Sharjah, United Arab Emirates*
¹⁶⁴*Department of Physics and Astronomy, University of Uppsala, Uppsala, Sweden*
¹⁶⁵*Department of Physics, University of Illinois, Urbana, Illinois, USA*
¹⁶⁶*Instituto de Fisica Corpuscular (IFIC), Centro Mixto Universidad de Valencia—CSIC, Valencia, Spain*
¹⁶⁷*Department of Physics, University of British Columbia, Vancouver, British Columbia, Canada*
¹⁶⁸*Department of Physics and Astronomy, University of Victoria, Victoria, British Columbia, Canada*
¹⁶⁹*Fakultät für Physik und Astronomie, Julius-Maximilians-Universität Würzburg, Würzburg, Germany*
¹⁷⁰*Department of Physics, University of Warwick, Coventry, United Kingdom*
¹⁷¹*Waseda University, Tokyo, Japan*
¹⁷²*Department of Particle Physics and Astrophysics, Weizmann Institute of Science, Rehovot, Israel*
¹⁷³*Department of Physics, University of Wisconsin, Madison, Wisconsin, USA*
¹⁷⁴*Fakultät für Mathematik und Naturwissenschaften, Fachgruppe Physik, Bergische Universität Wuppertal, Wuppertal, Germany*
¹⁷⁵*Department of Physics, Yale University, New Haven, Connecticut, USA*

^aDeceased.

^bAlso at Department of Physics, King's College London, London, United Kingdom.

^cAlso at Institute of Physics, Azerbaijan Academy of Sciences, Baku, Azerbaijan.

^dAlso at TRIUMF, Vancouver British Columbia, Canada.

^eAlso at Department of Physics, University of Thessaly, Greece.

^fAlso at An-Najah National University, Nablus, Palestine.

^gAlso at Department of Physics, University of Fribourg, Fribourg, Switzerland.

^hAlso at Department of Physics, Westmont College, Santa Barbara, California, USA.

ⁱAlso at Departament de Fisica de la Universitat Autònoma de Barcelona, Barcelona, Spain.

^jAlso at Affiliated with an institute covered by a cooperation agreement with CERN.

^kAlso at The Collaborative Innovation Center of Quantum Matter (CICQM), Beijing, China.

^lAlso at Faculty of Physics, Sofia University, "St. Kliment Ohridski," Sofia, Bulgaria.

^mAlso at Università di Napoli Parthenope, Napoli, Italy.

ⁿAlso at Institute of Particle Physics (IPP), Canada.

^oAlso at University of Colorado Boulder, Department of Physics, Boulder, Colorado, USA.

^pAlso at Borough of Manhattan Community College, City University of New York, New York, New York, USA.

^qAlso at National Institute of Physics, University of the Philippines Diliman (Philippines), Philippines.

^rAlso at Department of Financial and Management Engineering, University of the Aegean, Chios, Greece.

^sAlso at Centro Studi e Ricerche Enrico Fermi, Italy.

^tAlso at Institutio Catalana de Recerca i Estudis Avancats, ICREA, Barcelona, Spain.

^uAlso at Technical University of Munich, Munich, Germany.

^vAlso at Yeditepe University, Physics Department, Istanbul, Türkiye.

^wAlso at Institute of Theoretical Physics, Ilia State University, Tbilisi, Georgia.

^xAlso at CERN, Geneva, Switzerland.

^yAlso at Center for Interdisciplinary Research and Innovation (CIRI-AUTH), Thessaloniki, Greece.

^zAlso at Hellenic Open University, Patras, Greece.

^{aa}Also at Department of Physics, Stellenbosch University, South Africa.

^{bb}Also at Department of Physics, California State University, Sacramento, California, USA.

^{cc}Also at Département de Physique Nucléaire et Corpusculaire, Université de Genève, Genève, Switzerland.

^{dd}Also at Institut für Experimentalphysik, Universität Hamburg, Hamburg, Germany.

^{ee}Also at Department of Physics, Stanford University, Stanford, California, USA.

^{ff}Also at Institute for Nuclear Research and Nuclear Energy (INRNE) of the Bulgarian Academy of Sciences, Sofia, Bulgaria.

^{gg}Also at Washington College, Chestertown, Maryland, USA.

^{hh}Also at Institute of Applied Physics, Mohammed VI Polytechnic University, Ben Guerir, Morocco.

ⁱⁱAlso at Institute of Physics and Technology, Mongolian Academy of Sciences, Ulaanbaatar, Mongolia.